Modification of Back-Surface Contacts to Antimony Sulfide Active Layers Using Carrier-Selective Thionated Perylene Derivatives for Improved Photovoltaic Performance

WPI

A Major Qualifying Project Report

Submitted to the Faculty of

WORCESTER POLYTECHNIC INSTITUTE

in partial fulfillment of the requirements for the

Degree of Bachelor of Science in Chemical Engineering

By:

Curtis W. Doiron

Approved:

Professor Ronald L. Grimm,

Primary Advisor

Abstract

We hypothesized that sulfur-terminated organic perylene monolayers on silicon substrates would improve the solar energy conversion behavior of deposited antimony sulfide (Sb_2S_3) photoabsorbers. In particular, this study explored the effects of perylene and sulfur derivatives of perylene that were covalently attached to the silicon substrate for their ability to effect strong adhesion of Sb_2S_3 layers and to improve carrier transfer that would maximize solar energy conversion performance. Covalent attachment of perylene tetracarboxylic dianhydride to aminosilane surfaces was confirmed by anhydride and imide carbonyl features in surface IR measurements. We investigated the thionation of surface carbonyls in the exposed perylene anhydride functional groups by a variety of thionating reagents including Lawesson's Reagent (LR) and P_4S_{10}. X-ray photoelectron spectroscopy (XPS) quantified the degree of thiocarbonyl conversion as well as the presence of unwanted reagent decomposition byproducts. XPS results reveal the highest carbonyl-to-thione conversion and smallest side product contamination resulted from a treatment of P_4S_{10} under room-temperature conditions. Sb_2S_3 absorber layers were deposited by chemical bath onto silicon substrates with thioanhydride and thioester organic functionality, with non-thionated anhydride and ester control surfaces. Photoelectrochemical studies with the thianthrene$^{+/0}$ redox couple established the solar energy conversion performance of the resulting Sb_2S_3 thin film electrodes as a function of the chemistry of the interfacial layer between the Sb_2S_3 and the silicon substrate. Thioanhydride surfaces facilitated improved photovoltaic properties of deposited Sb_2S_3 layers compared to sulfur-free anhydride surfaces and resulted in a world record open-circuit voltage (V_{oc}) of –900 mV for Sb_2S_3 absorbers. We attribute the large V_{oc} to the combination of favorable sulfur-functionalized surfaces for deposition, charge transfer properties of the perylene layer, and use of the thianthrene$^{+/0}$ redox couple.

Contents

1. Introduction

For single absorber solar-cells, solar conversion efficiencies of promising materials are approaching theoretical maxima, with 26% reported for monocrystalline silicon, and above 20% reported for various sulfide and perovskite materials.[1] Stacking absorber cells with differing band gaps yields improved solar efficiency in so-called "tandem" cells (Figure 1), with efficiencies increasing to as high as 32% for two-layer devices. Limits to the efficiency of single-layer solar devices include the Shockley-Queisser limit,[2] which attempts to approximate realistic efficiencies due to imperfect interfaces and various losses.

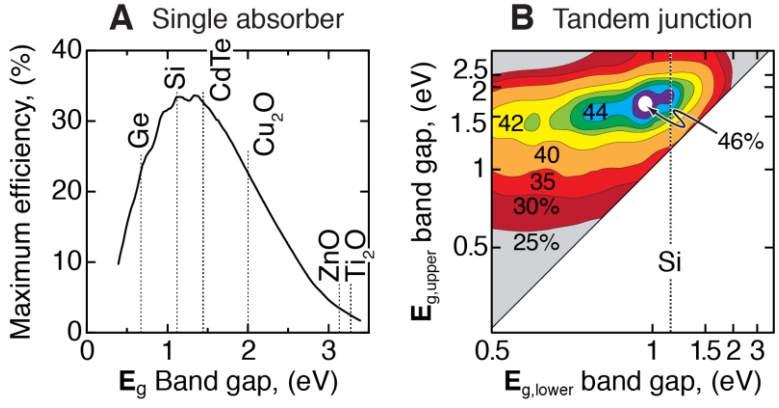

Figure 1: Theoretical efficiencies of single-absorber (A) and double-absorber tandem junction (B) solar cells as functions of material band gaps. The efficiency of a single-absorber cell maximizes at ~34% for band gaps between 1.1-1.5 eV. Materials such as Si and CdTe are well positioned for high efficiency (A). Adding a second absorber increases efficiencies to 44-45% for tandem arrangements with Si as the bottom absorber and a top absorber with a band gap of 1.6-1.8 eV (B).[3]

Promising materials to place in tandem with the well-studied monocrystalline silicon absorber layers are metal sulfides. Various sulfides, including tin sulfides, lanthanide sulfides, cadmium sulfide, copper sulfide, and antimony sulfide, as well as ternary and quaternary sulfides, have been studied extensively. Antimony sulfide, in particular, possesses the ideal 1.6-1.8 eV band gap to pair with silicon bottom absorbers;[4] this material is considered in the current study. Metal sulfide thin films may be prepared by a variety of methods,[5-7] but they may be deposited easily by aqueous chemical baths from metal cations and organosulfur precursors.[8-11] Varying deposition method,

deposition time, bath temperature, bath pH, annealing temperature, and/or annealing atmosphere adjusts various characteristics of the resulting films, including thickness, grain size, band gap, and photovoltaic properties.[7,8] Challenges involved in preparing competitive devices from these methods include carrier transport barriers at the interface and variance in conductivity of carriers between crystal dimensions; layered sulfides, in particular, feature much stronger bonds in-plane than out-of-plane, in which they may possess only van der Waals interactions with neighboring planes.

Depending on the orientation of the p-n junction, an interface layer with carrier-selective transport properties may improve device efficiency by preventing carrier recombination. TiO_2 appears attractive as a hole-blocking layer due to an extremely low valence band energy,[12] but the possibility of chalcogenide exchange with overlaying metal sulfide layers presents a concern for the longevity of such devices. Organic molecules pose attractive options as electron transport layers due to tunability of band positions and bandgap by varying substituents. The rylene dyes, including substituted naphthalenes, perylenes, terrylenes, and quaterrylenes, provide adjustable length from varying the number of naphthalene units, and adjustable bandgap from varying "bay" substituents[13] at C-H bond positions around aryl rings. Rylene dyes are used industrially as pigments and dyes, and a variety of inexpensive possible precursors are available from commercial vendors.

This work investigates the use of a well-studied rylene derivative, perylene tetracarboxylic dianhydride (PTCDA, see Figure 2, left side). The band positions of PTCDA suggest it may serve as a hole-blocking layer for the Si - Sb_2S_3 system. Procedures for synthesizing perylene derivatives from PTCDA first convert PTCDA to a di-imide or tetra-ester form to increase solubility in organic solvents.[14,15] From there, various "bay"-region reactions,[16,17] asymmetric substitution reactions at the carbonyls,[14] and thionation of various soluble derivatives[18,19] are possible.

Recent research may address the solubility issues of PTCDA. Kelber et al.[20] studied the mechanism for the formation of perylene tetra-esters (Figure 2) and found that DBU and alcohols generate a reactive ring-opened di-ester di-acid intermediate in solution. This reactive species undergoes ring-closing reactions with primary amines or opens to tetra-esters with addition of alkyl halides. These reactions represent possible anchoring methods to efficiently attach PTCDA to surfaces either by surface-attached alkyl halides to yield ester linkages, or by surface-attached amines to yield imide connectivity. Surfaces terminated with either alkyl halides or primary amines can form covalent bonds with the reactive perylene species to attach the perylenes to surfaces.

In regard to the route to link perylenes to surface through imide formation, amine-terminated surfaces have been prepared on monocrystalline, atomically flat Si (111) surfaces from Grignard attachment of allyl carbon chains, followed by halogenation and amination procedures (Figure 3).[21] A proposed method for testing the attachment and utility of perylene electron transport layers on surfaces is to prepare amine-terminated silane surfaces on oxidized silicon substrates. The silane reaction is known to go to highly ordered coverages for aliphatic aminosilanes.[22]

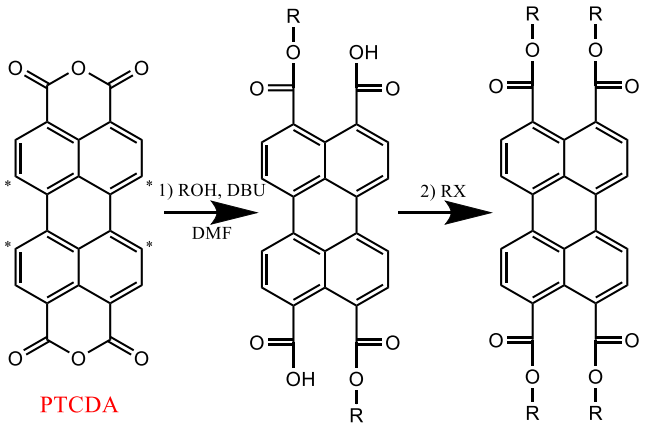

Figure 2: One-pot synthesis of perylene 3,4,9,10-tetracarboxylic tetraester from commercially available 3,4,9,10-tetracarboxylic dianhydride (PTCDA). So-called "bay" positions are indicated with asterisks. The first step of base-catalyzed ring-opening of the anhydride by 1,8-diazabyclo[5.4.0]undec-7-ene (DBU) with a primary alcohol brings the reactive diester diacid intermediate into solution. The reactive species may undergo further esterification with addition of the alkyl halide in the second step as pictured or undergo ring-closure with a primary amine with elimination of ROH.

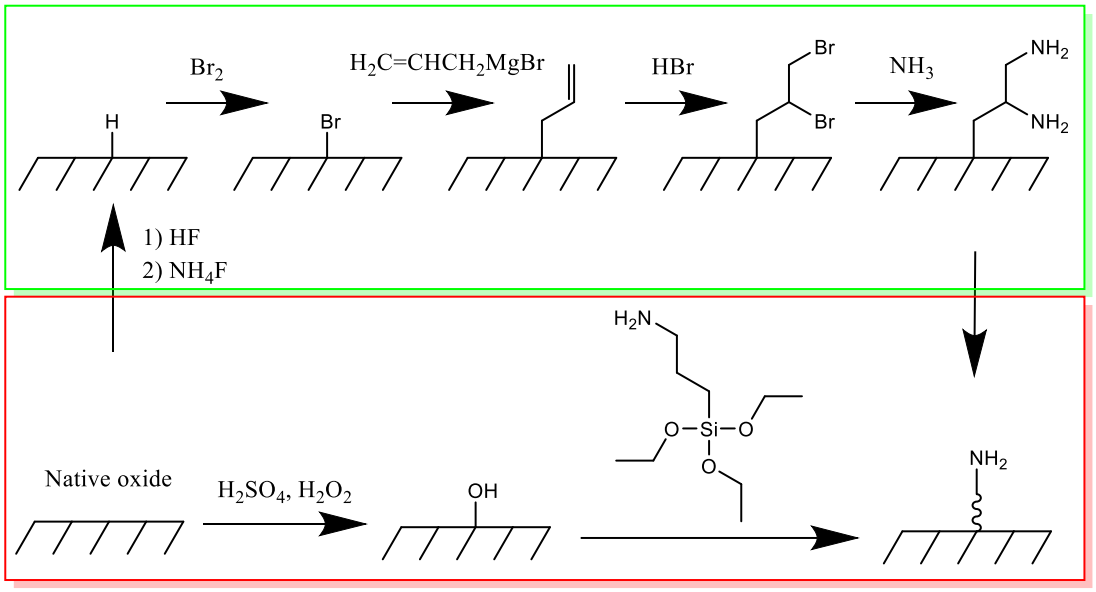

Figure 3: Preparation of amine-functionalized silicon surfaces by two methods. *Green/Top:* For single-crystalline silicon substrates, an HF/NH_4F etch generates an atomically flat air-sensitive H-terminated surface. The surface may then undergo halogenation and Grignard reactions to produce an alkylated surface with terminal halides, which are subjected to amination reactions with ammonia. *Red/Bottom:* Amine-terminated substrates may be prepared in air by chemical etching with piranha solution to produce a chemically oxidized surface, followed by silanization procedures with (3-aminopropyl)triethoxysilane. The bottom procedure produces amine-terminated oxidized silicon substrates for testing purposes while avoiding air free conditions.

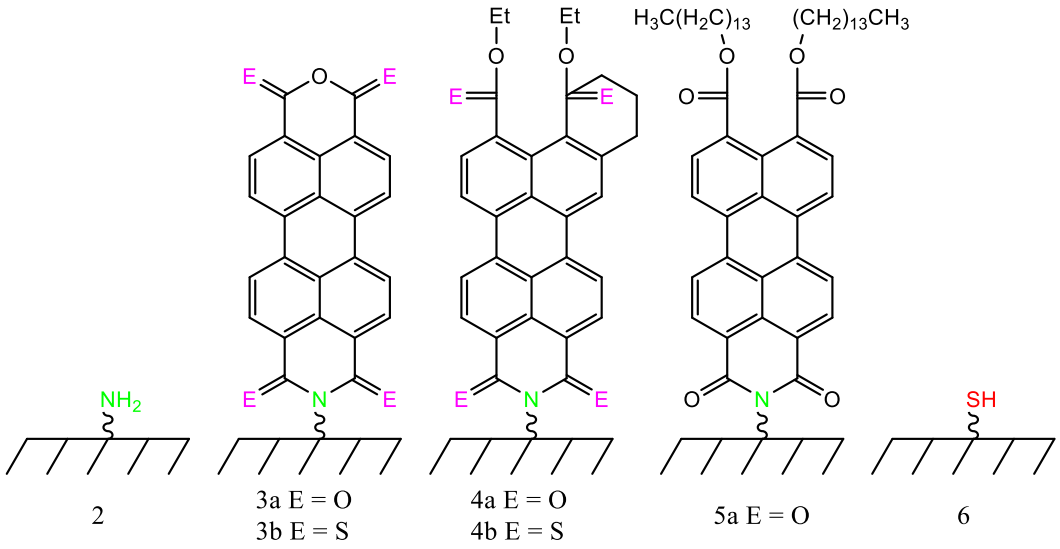

Figure 4: Surfaces **2**, **3a** and **3b**, **4a** and **4b**, **5a**, and **6**. **2** is an oxidized silicon substrate amine-functionalized by (3-aminopropyl)triethoxysilane for reaction with perylenes. **3a** is a surface where perylene 3,4,9,10-tetracarboxylic dianhydride has been covalently attached to the surface amine. **4a** is a surface where **3a** surfaces have been ring-opened on the top to ethyl ester moieties, following similar procedures for ring-opening for perylene attachment. **5a** is a surface where **3a** surfaces have been ring-opened on the top to tetradecyl ester moieties in a similar fashion. **6** is a surface that has been thiol-functionalized with 3-mercaptopropyltrimethoxysilane for comparisons of organosulfur layers. **3b** and **4b** are thionated derivatives of **3a** and **4a**, respectively, formed by immersion of **3a** and **4a** substrates in solutions of thionating reagents. Thionated derivatives of **5a** were not studied.

A desired trait of the perylene layer is to direct the growth of metal sulfides from bath deposition procedures. This work proposes several surfaces, terminating in either carbonyls (**3a**, **4a**) or thiocarbonyls (**3b**, **4b**) (Figure 4), for testing of bath-deposited metal sulfide thin films. Preparation of sulfur-functionalized perylene surfaces may be accomplished either by attachment of thionated perylenes or by thionation of existing perylene surface species. The insolubility of the PTCDA precursor has prevented immediate modification of the anhydride carbonyls to thiocarbonyls to date. A similar molecule, naphthalic anhydride, has been successfully converted to di-thio and tri-thio anhydrides by reactions with thionating reagents such as Lawesson's Reagent (LR) in boiling toluene or chlorobenzene,[23-25] with an intermediate step of base-catalyzed ring-flip (Figure 5). Besides LR,[26] other thionating reagents such as P_4S_{10} [27] and a P_4S_{10}-pyridine complex[28,29] have been used for solution thionations in organic chemistry.

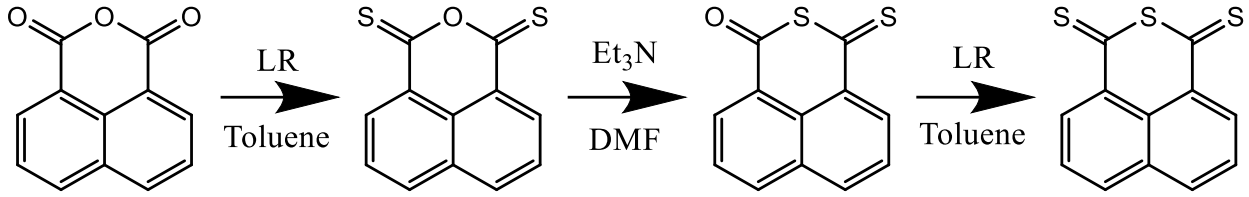

Figure 5: Established procedure[22-24] for thionation of 1,8-naphthalic anhydride to trithio-1,8-naphthalic anhydride. While published procedures use a three-step procedure to convert both carbonyls and the ether oxygen to sulfur atoms, this work considers only the first step – the use of thionating reagents in aromatic solvents.

While thionation procedures are typically conducted in refluxing aromatic solvents for prolonged times,[26,27] these harsh reaction conditions cause concerns for the stability of monocrystalline silicon substrates. While this work uses oxidized silicon substrates for attachment and photoelectrochemical studies, future work on monocrystalline silicon will include restrictions on high temperature to preserve the electronic properties of the silicon. To this end, we restricted the thionation reaction temperatures to milder conditions in this work.

The **long-term goal** of this research path is a thionated perylene linker layer that supports metal sulfide deposition and provides carrier-selective transport for single-

crystalline silicon / metal sulfide tandem solar cells. This project aims to initiate several research pathways (Figure 6): prepare amine-functionalized oxidized silicon surfaces (**2**), attach perylene molecules to the amine-functionalized surfaces through various methods (**3a**), attack several synthetic difficulties in preparing thionated perylene surfaces (**3b**, **4b**), and test whether the thionated perylene surfaces improve photovoltaic properties of attached metal sulfides. Infrared reflection-absorbance spectroscopy (IRRAS) quantifies the presence of phenyl stretches and formation of imide bonds upon attachment of the perylene molecule to amine-functionalized surfaces. IRRAS also confirmed ring-opening of surface anhydrides to di-ester groups (**4a**, **5a**) through carbonyl C=O stretches. After thionation procedures to form **3b** and **4b**, X-ray photoelectron spectroscopy (XPS) measured the coverage of sulfur and phosphorus to compare the effectiveness of thionation strategies. Deposited metal sulfides were examined by XPS and tested by photoelectrochemistry (PEC) with non-aqueous redox couples.

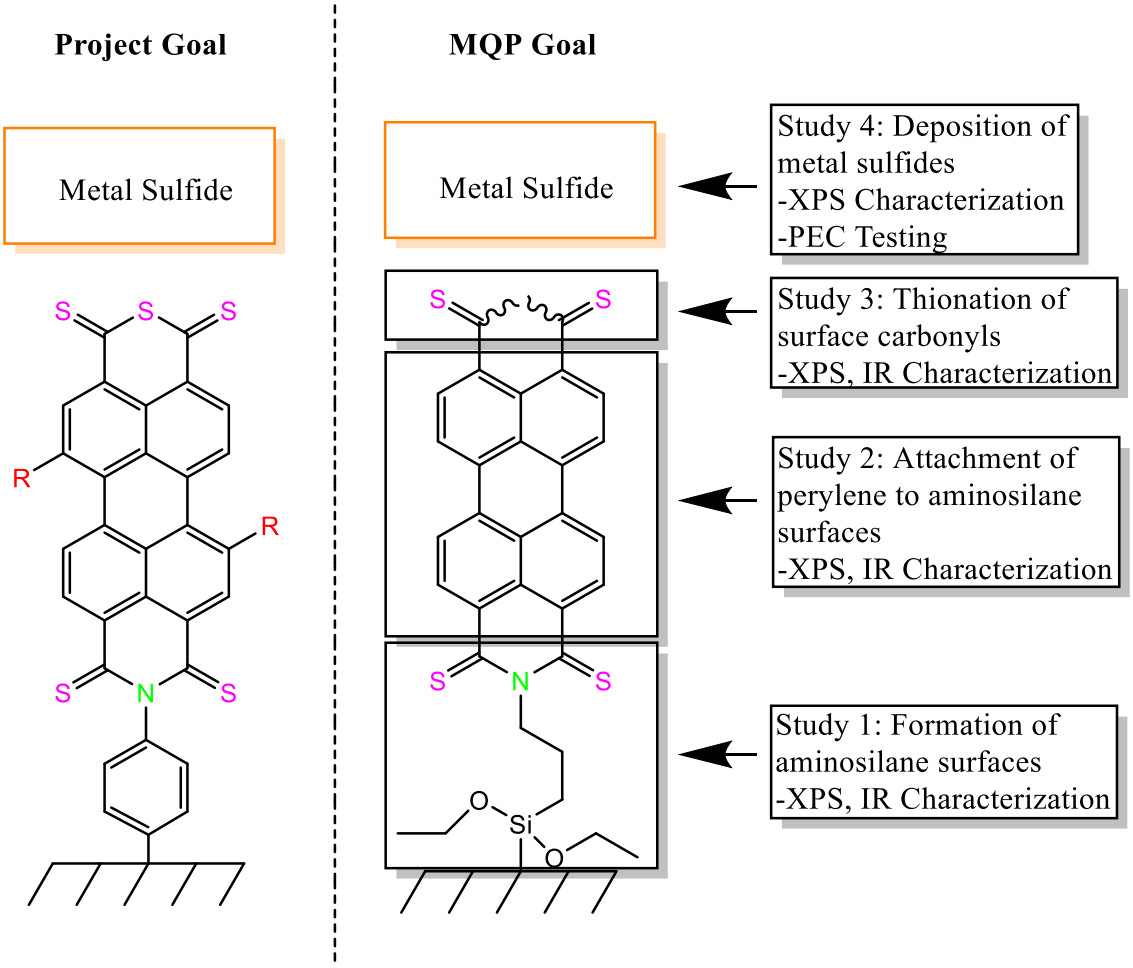

Figure 6: Comparison of long-term project goal (left) with current MQP project goal (right). While future work will utilize single-crystalline silicon substrates with Grignard-attached phenylamines to anchor modified perylenes to surfaces (left), this project will study various aspects of attaching perylenes to amine-functionalized surfaces and follow up with thionation procedures (right). XPS and IR spectroscopy will confirm the progress of surface modification through Studies 1-3. XPS will examine deposited metal sulfide films in Study 4, and various carbonyl and thiocarbonyl species will be tested for improvement of electrical properties by photoelectrochemical experiments.

2. Experimental Section

2.1. Inert Atmosphere Environments

A Schlenk line with a base pressure of <1 mtorr was used for freeze-pump-thaw cycles on dichloromethane (DCM) and vacuum distillations of pyridine and toluene. Following freeze-pump-thaw cycles or vacuum distillations, the solvent head space was back-filled with Ar (UHP, Airgas) for transfer to other inert atmosphere environments. The Schlenk line was also used to provide Ar pressure for cannula transfer of dry toluene to sealed sonication tubes, and for airfree removal of solvent after sonication procedures.

A N_2-filled (UHP, Airgas) glovebox with <0.5 ppm O_2 was used for storage of redox couples, storage of various dry solvents and air-sensitive solids, and for photoelectrochemical experiments.

A flushbox purged with house-generated N_2 with 1 ± 1% O_2 was used for storage of various dry solvents and air-sensitive solids, as well as thionation reactions. A water-free atmosphere was assumed in the flushbox.

2.2. Chemicals

All water used was provided by a Millipore Milli-Q system at 18 MΩ cm resistivity. H_2SO_4 (technical grade, Fisher), H_2O_2 (35 wt%, Alfa Aesar), HCl (ACS reagent, Alfa Aesar), HNO_3 (68-70 wt%, ACROS Organics), *N*,*N*-dimethylformamide (DMF, 99.8+%, Alfa Aesar), $CHCl_3$ (99+%, ACROS Organics), acetone (certified ACS, Fisher), ethanol (denatured, 91.6%, 3.7% methanol, 1.9% MIBK, 1% heptane, 1% ethyl acetate, 1% toluene, Alfa Aesar), bromoethane (98%, Alfa Aesar), 2-propanol (99.9%, Fisher), 1-butylamine (99%, Alfa Aesar), 1-butanol (99.5%, ACROS Organics), 1-tetradecanol (Aldrich), 1-bromotetradecane (97%, Alfa Aesar), ammonium hydroxide (28% aqueous, Alfa Aesar), 1,8-diazabycyclo[5.4.0]undec-7-ene (DBU, 98+%, ACROS Organics), perylene 3,4,9,10-tetracarboxylic dianhydride (PTCDA, 97%, Aldrich), and antimony potassium tartrate hydrate (98%, Alfa Aesar) were stored in air and used as received. The two silanes used,

(3-aminopropyl)triethoxysilane (APTES, ≥98.0%, Aldrich), and (3-mercaptopropyl)trimethoxysilane (≥80%, Aldrich), were opened and stored in air, but were briefly flushed with an Ar stream before sealing. P_4S_{10} (98+%, ACROS Organics) and Lawesson's Reagent (LR, 99%, ACROS Organics) were opened and stored in the flushbox and used as received. $LiClO_4$ (battery grade, 99.99%, Sigma-Aldrich) and tetrabutylammonium perchlorate (for electrochemical analysis, Sigma-Aldrich) were opened and stored in the glovebox and used as received.

Thioacetamide (99+%, ACROS Organics) was prepared to a 0.1 M aqueous stock solution. Triethanolamine (97%, ACROS Organics) was prepared to a 50% v/v aqueous stock solution. Silico-tungstic acid hydrate (≥99.9%, Aldrich) was prepared to a $1x10^{-5}$ M aqueous stock solution. All aqueous stock solutions were stored in air.

Methanol (99.8+%, Alfa Aesar) and toluene (99.7+%, Alfa Aesar) for sonication procedures and silane reactions were dried and stored over molecular sieves (3Å, Alfa Aesar) in ambient atmosphere. Commercial extra-dry septum-sealed toluene (99.85%, extra dry over molecular sieves, ACROS Organics) was used specifically for airfree sonication procedures. Commercial extra-dry septum-sealed chlorobenzene (99.8%, extra dry, ACROS Organics) was used for solution thionation reactions.

DCM (certified ACS, stabilized, 99.9%, Fisher) and diethyl ether (99.9%, Fisher) were subjected to three cycles of freeze-pump-thaw on the Schlenk line before back-filling with Ar. Molecular sieves were added to the DCM in the flushbox and the solvent was dried for three days before use. Molecular sieves were added to the diethyl ether in the glovebox and the solvent was dried for three days before use. Toluene (99.7+%, Alfa Aesar) and pyridine (ACS reagent, Phamco-AAPER) for thionation reactions were vacuum distilled from CaH_2 (93%, ACROS Organics) into a receiver flask containing activated molecular sieves. The solvents were allowed to dry for three days before use. Acetonitrile for photoelectrochemical experiments was obtained from an in-house solvent drying system.

Ferrocene (98%, Aldrich), acetylferrocene (97%, Alfa Aesar), and thianthrene (98%, Frontier Scientific) were separately purified by vacuum sublimation on the Schlenk line and transferred to the glovebox under Ar before use. Ferrocenium tetrafluoroborate (technical grade, Sigma-Aldrich) was recrystallized from a diethyl ether / acetonitrile mixture and degassed under vacuum on the Schlenk line.

Acetylferrocenium tetrafluoroborate was synthesized in the glovebox by Clare Masucci as part of her MQP work in the Grimmgroup.[30] Synthetic procedures may be found in full in that report. Briefly, 390 mg acetylferrocene and 320 mg $AgBF_4$ (99%, ACROS Organics) were combined in 150 mL diethyl ether. The ether was evaporated, and the solid was dissolved in 100 mL DCM. The solution was then filtered through PVDF syringe filters (13mm, 0.10μm pore size, Advangene) to recover the soluble species. The solution was concentrated to ~5 mL by heating, then 100 mL diethyl ether was added. The solid was recrystallized from this solution to produce dark blue crystals. Nonaqueous redox testing and silicon PEC experiments confirmed successful synthesis and purification.

Thianthrene tetrafluoroborate was synthesized following a literature reaction of thianthrene and nitrosonium tetrafluoroborate ($NOBF_4$, 97%, ACROS Organics, used as received) in acetonitrile and precipitated with diethyl ether.[31] Departing from the published methodology, we conducted the synthesis in a nitrogen-purged glovebox with freshly sublimed thianthrene in 5% molar excess with the $NOBF_4$. Our rationale was that thianthrene tetrafluoroborate is later mixed with thianthrene in the redox solution; thus, any unreacted thianthrene in the oxidation reaction with $NOBF_4$ would not represent a contaminant necessitating separation / extraction / purification. The dark blue solid was dried under vacuum and thus used without further purification.

2.3. X-ray Photoelectron Spectroscopy (XPS) Methods

A PHI5600 XPS system, described in previous publications,[21] acquired XPS data scanning the polished side of surfaces **2**, **3a**, and **3b**, as well as deposited Sb_2S_3 thin films. No substrates required charge neutralization due to use of conductive n^+-Si substrates and sufficient conductivity in the Sb_2S_3 thin films. The UHV chamber pressure remained $< 5 \times 10^{-9}$ torr during scans. Wide-energy-range surveys of each sample determined the elements present on the substrates that were supplemented by high-resolution scans of the C 1s, O 1s, N 1s, S 2s, S 2p, P 2p, and Sb 3d regions. All features were fit to GL(30) peak shapes with various backgrounds: the C 1s, O 1s, N 1s, S 2s, and S2p, employed linear-shaped backgrounds, while the P 2p and Sb 3d region employed Shirley-shaped backgrounds. Features in the C 1s, O 1s, N 1s, S 2s, S 2p, and P 2p regions were constrained to identical full-width-at-half-maximum (fwhm) values for each element. Features in the Sb 3d region assigned to oxygen species (due to overlapping regions with O 1s) were mutually constrained to identical fwhm values, while other features assigned to Sb species were constrained to a separate fwhm value. The peak separation of the S 2p and P 2p doublets were respectively set at 1.18 eV and 0.84 eV, and the peak separation of the Sb 3d doublet was set at 9.34 eV, per literature values.[32]

A thermal stability study on surface **3a** employed an in-situ heater to encourage desorption of adventitious organic species present on all samples studied. The temperature of the sample was increased to 200 ˚C in the XPS vacuum over the course of 20-30 minutes, after which the temperature was maintained for an hour. After shutting off the heater, the sample gradually cooled down to ~30 ˚C over the course of another hour. Wide-field XP survey spectra and high-resolution scans of the C 1s, O 1s, N 1s, and Si 2p regions were acquired both before and after the heating study for comparison.

2.4. Infrared Reflection-Absorption Spectroscopy (IRRAS) Methods

Surface IR measurements were performed on a Bruker Vertex 70 (Bruker, Billerica, MA) instrument equipped with a liquid-N_2-cooled MCT detector and an AutoSeagull accessory with variable polarizer (Harrick Scientific, NJ). The Autoseagull accessory was purged with house-generated "dry" N_2 gas containing 1 ± 1 % O_2. Measurements were conducted at 40° and 80° with respect to the surface normal in S and P polarization. Backgrounds and scans of **2**, **3a**, **3b**, **4a**, **4b,** and **5a** surfaces on p-Si were conducted in a transflection geometry by placing substrates on top of ~0.5mm spacers on top of a gold mirror. Later measurements of the same sample occurred with the substrate in the same approximate position as with background acquisitions, and the accessory's atmosphere controlled to equalize water vapor influence as compared to each background scan. Surface IR results presented are 512-scan averages of **3a** or **5a** surfaces with a subtracted background of **2**. Full IR spectra of **3a** and **5a** surfaces are provided in the appendix (Figures A3 and A4).

To assign peaks in the surface IR scans to specific carbonyl and C-H features from positions, various perylene derivatives were synthesized (see 2.14). Powder scans were conducted using the same instrument, but the setup utilized a GoldenGate diamond ATR accessory and a deuterated lanthanum α alanine-doped triglycine sulphate (DLaTGS) detector. Powder scans reported are averages of 512 scans with an air background. Full IR spectra of all compounds synthesized for this purpose are provided in the appendix (Figures A5-A7).

2.5. Photoelectrochemistry (PEC) Methods

The thianthrene$^{+/0}$ redox couple was tested by reference to the $Ag^{+/0}$ electrode. The cell was prepared by first dissolving the supporting electrolyte $LiClO_4$ to 1M in 15 mL acetonitrile. Separately and in an air ambient, a silver wire (99.999%, Alfa Aesar) was cleaned by mechanical abrasion with 1200-grit sandpaper, rinsing in water, a 10 s

submersion in a 10 vol % $HNO_{3(aq)}$ solution, further rinsing, and drying. The silver wire was threaded partway through a sealing septum and transferred to the glovebox.

To construct the $Ag^{+/0}$ reference electrode, an aliquot of the $LiClO_4$/acetonitrile mixture was removed and added to a 6 mm O.D. borosilicate tube with a Vycor fritted bottom (held in place with solvent-inert heat shrink tubing). Two grains of $AgNO_3$ (>99.9%, Alfa Aesar, dried at 100 °C under vacuum) were dissolved in the solution. The silver wire and septum were positioned such that the cleaned portion was submerged in the silver nitrate solution with a portion of wire protruding from outside of the septum-sealed electrode for electrical connection to the potentiostat.

In the electrochemical cell, 119 mg thianthrene and 4 mg thianthrene tetrafluoroborate were added. A platinum wire served as the working electrode and a platinum mesh served as the counter electrode. Open-circuit potential measurements established the cell potential, E_{cell}, versus $E_{Ag^{+/0}}$. Cyclic voltammograms acquired at 50 mV s^{-1} established the thianthrene$^{+/0}$ Nernstian formal potential, $E^{o\prime}$, versus $E_{Ag^{+/0}}$. As the silver/silver ion reference electrode employed nonstandard concentrations (two grains is not a standard concentration), the addition of ferrocene$^{+/0}$ and acetylferrocene$^{+/0}$ redox couples aided in determining the redox potential of the thianthrene$^{+/0}$ redox couple in reference to the well-established metallocene redox potentials.

Degenerately arsenic-doped n-type silicon substrates with **2**, **3a**, **3b**, **4a**, **4b**, or **6** surfaces, with antimony sulfide deposited, were converted to electrodes for photoelectrochemical experiments. Substrates were mounted by off scratching deposited sulfide, if any, from the unpolished back, then adhering with eutectic GaIn, prepared from melting Ga (99.99%, Strem) and In (99.9999%, Alfa Aesar) together in appropriate proportions, to copper wire. The electrical connection was stabilized with conductive silver paint (SPI Supplies, 05002-AB) before covering all exposed back contact features with chemically inert 9460™ epoxy (Henkel Loctite Hysol) until only the desired active

electrode area remained uncovered. The epoxy was cured for the recommended time of 3 days at ambient conditions or overnight in a 100 ˚C oven. Immediately before the electrodes were transferred to the glovebox, each mounted electrode was immersed vertically in 10% aqueous HCl for 10 seconds to remove surface antimony oxide species, then rinsed with copious water and dried under a flowing stream of Ar.

To test the Sb_2S_3 thin films, 1 M $LiClO_4$ or 0.2 M tetrabutylammonium perchlorate, ~30 mM thianthrene, and ~2 mM thianthrene tetrafluoroborate were dissolved in 10 mL acetonitrile by magnetic stirring in a photoelectrochemical cell in the glovebox, resulting in a dark purple solution. A Pt wire (99.997%, Alfa Aesar) reference electrode and a Pt gauze (99.9%, Alfa Aesar) counter electrode, both previously cleaned by a ten second immersion in freshly prepared aqua regia solution (3:1 v/v HCl:HNO_3) were lowered into the solution, while positioned to avoid mutual contact. A test electrode was lowered into the solution and suspended with ~1mm of solution between the exposed surface and the glass bottom of the photoelectrochemical cell. This positioning enabled redox charge transfer while obviating possible collisions with the stir bar and strong solution absorption effect. The magnetic stir bar was positioned to provide robust stirring without obstructing light from the lamp entering the cell.

Over the course of photoelectrochemical experiments, the thianthrene tetrafluoroborate in the redox solution depleted slowly, as judged from a gradual color change of the redox solution from dark purple to pale purple. Considering the white color of thianthrene^0 and the dark purple color of thianthrene$^+$, we ascribe this color change to the slow reduction of the strongly oxidizing thianthrene$^+$ species that was perhaps due to trace water on the electrodes, glassware, or elsewhere. Additional thianthrene tetrafluoroborate was added intermittently to maintain an approximate consistent concentration, as determined from a consistent color of the redox solution. The dynamic absorbance of the solution therefore presents a possible source of error.

A 300 W ELH tungsten-halogen lamp simulated 100 mW cm^{-2} Air Mass 1.5 Global "1 sun" illumination. A potentiostat (SP-300, Bio-Logic, Seyssinet-Pariset, France) scanned open-circuit voltage and cyclic voltammogram programs. For each electrode, an open-circuit voltage sequence ran for 30 seconds during which the voltage was recorded for the electrode in the absence and in the presence of illumination to provide a comparison of light and dark voltage. Stray light from ambient sources may have contributed to anomalously large "dark" voltages. Cyclic voltammograms were measured against the immersed platinum wire reference electrode, which was poised at the solution cell potential, E_{cell}. Cyclic voltammograms scanned from –0.9 V to +0.4 V, reverse scanned to –1.0 V, and finally scanned forward and ended at –0.9 V under illumination, and then a separate cyclic voltammogram was collected with the light switched off to provide a measurement of photo-response.

2.6. Nuclear Magnetic Resonance (NMR) Spectroscopy Methods

A series of molecules were synthesized for IR analysis for the interpretation of the surface spectra and for confirmation of thionation products. Separately, ^{1}H NMR spectra were acquired of these compounds to verify successful synthesis and purity that would otherwise limit the usefulness of such IR comparisons. All ^{1}H NMR spectra were recorded in $CDCl_3$ (99.8 atom% D, ACROS Organics) using a Bruker Avance AVIII NMR spectrometer at 500 MHz. ^{31}P NMR spectra were recorded in $CDCl_3$ using the same instrument at 202 MHz. ^{1}H NMR spectra were calibrated with reference to an internal standard of tetramethylsilane at 0.00 ppm and the residual solvent peak at 7.26 ppm. Reported NMR shifts exclude small features assigned to trace water and solvents.

*2.7. Chemically Oxidized Si(111) Substrates (**1**)*

Single-sided polished, 525 ± 15 μm thick, ≤0.006 Ω cm resistivity, degenerately arsenic-doped n^+-Si(111) substrates 1 × 1 cm or larger, for XPS analysis and photoelectrochemical experiments, or double-sided polished, 525 ± 25-μm thick, 0.10–0.12 Ω cm resistivity,

boron-doped p-Si(111) (EL-CAT Inc.) substrates 1 × 3 cm or larger, for IRRAS analysis, were cut from fresh wafers. After rinsing the substrates in water, the substrates were treated with freshly prepared 3:1 v/v conc. H_2SO_4 / 35% $H_2O_{2(aq.)}$ (piranha solution) for 10 minutes, with occasional tapping to dislodge gas bubbles from substrates. The substrates were then rinsed with copious water and dried under a flowing stream of Ar (UHP, Airgas).

*2.8. Study 1: Formation of Aminosilane Surfaces (**2**)*

Initially, 20 μL (3-aminopropyl)triethoxysilane was added by plastic-tipped autopipette to 10 mL dry toluene without stirring. The silane solution was mixed and then pipetted to cover substrates, each in its own test tube. The test tubes were sealed with parafilm and heated in a 60 ˚C oil bath for four hours.

Upon conclusion of the reaction, the solution was decanted, and the substrates were transferred to clean individual test tubes. The substrates were sonicated five minutes each in fresh toluene, acetone, methanol, and water, with rinses of acetone in between sonication steps. The substrates were then dried by a flowing stream of Ar and saved in dry plastic centrifuge tubes until further reaction.

*2.9. Study 2: Attachment of Perylene to Aminosilane Surfaces (**3a**)*

A reactive perylene solution[20] was prepared for immersion of substrates by dissolving 1 g PTCDA in 6 mL DMF, 1 mL ethanol, and 1 mL DBU under magnetic stirring at 60 ˚C for 30 minutes in air. The solution was diluted to 50 mL with DMF and immediately transferred, by pipette, to test tubes, each containing one aminosilane surface (**2**) to prevent scratching. The test tubes were then sealed with parafilm and immersed in an oil bath at 60 ˚C for 72 hours.

Upon conclusion of the reaction, the solution was decanted, the substrates were rinsed in acetone twice, and the substrates were transferred to clean individual test tubes. The substrates were sonicated five minutes each in toluene, acetone, methanol, and water,

with rinses of acetone in between sonication steps. The substrates were then dried by a flowing stream of Ar and saved in dry plastic centrifuge tubes until further reaction or examination by instrumentation.

*2.10. Perylene Bis(Ethyl Ester)-Terminated Surfaces (**4a**)*

A solution of 15 mL DMF, 0.3 mL ethanol, 0.3 mL DBU, and 0.3 mL bromoethane was prepared in air. The solution was then poured over anhydride surfaces (**3a**) in test tubes until the substrates were completely covered by the solution. The test tubes were then sealed with parafilm. Due to the low boiling point of bromoethane, the reaction was kept at room temperature. After 16 hours, the liquid was decanted. The substrates were sonicated five minutes each in toluene, acetone, methanol, and water, with rinses of acetone in between sonication steps. The substrates were then dried by a flowing stream of Ar and saved in dry plastic centrifuge tubes until further reaction or examination by instrumentation.

*2.11. Perylene Bis(Tetradecyl Ester)-Terminated Surfaces (**5a**)*

A solution of 1 mL 1-bromotetradecane, 1 mL DBU, and 1 g 1-tetradecanol in 10 mL DMF was prepared in air. The solution was then poured over perylene dianhydride surfaces (**3a**) in test tubes until the substrates were completely covered by the solution. The test tubes were then sealed with parafilm and immersed in a 60 ˚C oil bath for 16 hours. Following decanting, the substrates were sonicated five minutes each in toluene, acetone, methanol, and water, with rinses of acetone in between sonication steps. The substrates were then dried by a flowing stream of Ar and saved in dry plastic centrifuge tubes until further reaction or examination by instrumentation.

*2.12. Study 3: Thionation of Surface Carbonyls (**3b** from **3a**, **4b** from **4a**)*

This study explored the efficacy of carbonyl thionation to reveal which reagent yielded the highest thionation yield with minimal adsorbed byproducts such as oxidized

phosphorus species for the conversion of surface **3a** to **3b**. Thionating reagents and reaction solvents included Lawessons's reagent (LR) in toluene, P_4S_{10} in toluene, P_4S_{10} in DCM, and a pyridine-P_4S_{10} complex in pyridine. The conversion of **4a** to **4b** only utilized P_4S_{10} in toluene as that yielded optimal conversion properties among the various thionation reagents explored in the conversion of **3a** to **3b**.

The pyridine-P_4S_{10} complex was synthesized according to a literature procedure,[28] though our synthesis was conducted in a flushbox. In the flushbox, 4.45 g P_4S_{10} was added to 65 mL dry pyridine and heated to 110 °C for an hour. Yellow solid deposited from the solution upon cooling. The solution was vacuum filtered in the flushbox to recover the solid. The solid was sealed in a Schlenk flask under the flushbox atmosphere and transferred to the Schlenk line, where it was dried under vacuum. While the literature procedure recommends further purification to remove pyridine and residual P_4S_{10}, these species are not contaminants in our thionation procedures; our thionation scheme for the pyridine-P_4S_{10} complex uses pyridine as the solvent.

All thionation procedures were conducted in the flushbox, described above, under an active flow of 10 L min^{-1} "dry" N_2 gas.

Surfaces **3a** or **4a** were placed vertically into clean glass test tubes in the flushbox. Supersaturated solutions of the thionating reagent were prepared, consisting of ~50 mg of thionating reagent per 20 mL of dry solvent equilibrated by three minutes of vigorous magnetic stirring at room temperature. The solutions were then added by pipette to the substrates in the test tubes until the substrate was completely immersed; such volume was typically ~4 mL of solution. The test tubes were then sealed with rubber septa or parafilm and left upright at room temperature in the flushbox for a minimum of 48 hours.

To prevent deposition of oxidized phosphorus and sulfur species on substrate surfaces from decomposition of thionating reagents upon exposure to water or air, the substrates were cautiously cleaned post-thionation using an extensive sonication procedure with dry solvents. Experiments with less rigorous rinsing procedures resulted

in significant XPS-detected quantities of unwanted reagent byproducts that we will not discuss further. We report the methodology that yielded the highest coverage of desired species with minimal byproducts. Substrates were removed from the thionation solution in the flushbox, rinsed with fresh dry toluene in the flushbox, and sealed by septa into fresh test tubes, containing fresh dry toluene, to avoid contact with air during transfer to the Schlenk line. The sealed test tubes were then removed from the flushbox and placed into a sonication bath for five minutes. After sonication, the solution was diluted 3–5× with fresh dry toluene added by cannula under an inert atmosphere of Ar gas, then excess solvent was removed by cannula to keep the substrate only just fully immersed. The dilution and removal of the solvent was conducted to sonicate the substrate in a steadily decreasing concentration of thionating reagent to remove decomposition byproducts, while minimizing formation of oxidized phosphorus and sulfur species, which could adhere to the surfaces in the absence of solvent. The substrates were always immersed in solvent to minimize deposition of these species. After the dilution and removal process was complete, the substrates were sonicated for five minutes in fresh solvent. The process of diluting the solvent, removing solvent, and sonicating in new solvent was repeated twice to ensure that only trace air- and water-sensitive species remained.

Following air-free rinsing and sonication, the substrates were subjected to a sonication procedure in air, consisting of five minutes each in toluene, methanol, acetone, and water. The substrates were then dried by a flowing stream of Ar and placed in dry plastic centrifuge tubes until further reaction or examination by instrumentation.

2.13. Study 4: Deposition of Metal Sulfides

Sb_2S_3 depositions proceeded based on established procedures.[11] In a typical procedure, 1 g antimony potassium tartrate hydrate was dissolved in 15 mL water. Then, 6 mL 50% triethanolamine (aqueous) was added by autopipette, followed by 1.8 mL 28% NH_3 (aqueous), 15 mL 0.1 M thioacetamide (aqueous), and 3 mL 1×10^{-5} M silico-tungstic acid

(aqueous), before diluting to 48 mL with water, all under magnetic stirring at room temperature. The mixture was then pipetted into test tubes, each containing one substrate for deposition. The test tubes were then covered in parafilm and immersed in an oil bath at 40 ˚C for 40–48 hours.

After deposition, the solution was poured off, and the substrates were removed from the deposition without touching the faces and placed into an annealing furnace equipped with an Ar purge flow. After purging the atmosphere from the furnace, the furnace was heated to 300 ˚C over the course of 5 minutes, all while purging with a slow flow of Ar. After 30 min, the furnace was shut off and allowed to cool to room temperature before removal of the Ar stream and removal of the substrates from the furnace. Following annealing, the substrates appeared to be covered with dark grey films.

Substrates were deposited and annealed a second time using the same procedure as above to generate thicker films, as previous attempts had showed poor adhesion and photovoltaic properties with only a single deposition procedure. Following the second procedure, the substrates were stored in clean plastic centrifuge tubes until further use.

2.14. Synthesis of Perylene Derivatives for Comparisons of Powder and Surface IR

N,*N*′-dibutyl perylene-3,4,9,10-tetracarboxylic diimide was synthesized by a literature procedure[14] to aid in the interpretation of carbonyl-IR features from surfaces **3a** and **4a**, as described below. Perylene-3,4,9,10-tetracarboxylic tetraethyl ester and perylene-3,4,9,10-tetracarboxylic tetratetradecyl ester were synthesized using a modified literature procedure[17,20] to aid in the interpretation of carbonyl-IR features from surfaces **3a** and **4a**, as described below. Full NMR spectra are provided in the appendix for perylene-3,4,9,10-tetracarboxylic tetraethyl ester and perylene-3,4,9,10-tetracarboxylic tetratetradecyl ester.

To synthesize *N*,*N*′-dibutyl perylene-3,4,9,10-tetracarboxylic diimide, 3 mL 1-butylamine was added to a suspension of 1.330 g PTCDA in ~50 mL 1-butanol, and the solution was heated to reflux. After 90 minutes, the red solution had turned purple-

brown and no more suspended PTCDA was visible. Ice water (~50 mL) was added, and the solution was vacuum filtered to recover a purple-brown precipitate. The solid was washed with water, then it was dried in an oven at 100 ˚C overnight. Although literature procedures recommend column chromatography to remove residual PTCDA, IR analysis revealed no anhydride features, so no further purification was carried out. Insolubility to concentrations required for NMR prevented such analysis. Yield 1.486 g (87%). IR (cm^{-1}): 2959, 1691, 1652, 1592, 1336, 809.

To synthesize perylene tetracarboxylic tetraethyl ester, 2 g PTCDA, 2.26 mL DBU, and 1.75 mL ethanol were combined in 30 mL DMF at room temperature. Over the next half hour, the suspended PTCDA dissolved with formation of the soluble di-acid di-ester perylene derivative. Then, 2.23 mL 1-bromoethane was added to the solution with an additional 30 mL DMF. After stirring for an additional 90 minutes at room temperature, the solution was dark orange but lacked precipitate as reported in the literature when synthesizing a tetrabutyl ester derivative; this observation is due to differing solubility of the product when changing from butyl to ethyl groups. Water was added until the product precipitated, and then the solution was vacuum filtered to recover the orange precipitate. The solid was washed with ~100 mL water to remove residual DMF before drying in an oven at 100 ˚C overnight. Column chromatography was not performed due to adequate purity, as observed in the NMR (Figure A1). Yield 2.522 g (92%). ^{1}H NMR ($CDCl_3$): 7.93 (d, 4H), 7.86 (d, 4H), 4.41 (m, 8H), 1.45 (t, 12H).

To synthesize perylene tetracarboxylic tetratetradecyl ester, 2 g PTCDA, 2.26 mL DBU, and 6.42 g 1-tetradecanol were combined in 30 mL DMF at 60 ˚C. Over the next half hour, the suspended PTCDA dissolved with formation of the soluble di-acid di-ester perylene derivative. Then, 9 mL 1-bromotetradecane was added to the solution with an additional 30 mL DMF. After stirring for an additional 90 minutes, the solution was thick with orange precipitate. Additional water (~30 mL) was added, and then the solution was vacuum filtered to recover the orange precipitate. The solid was washed with ~100 mL

water to remove residual DMF before drying in an oven at 100 ˚C overnight. The solid melted overnight. Column chromatography (silica, 100% $CHCl_3$) removed trace impurities of reactants (Figure A2). Yield 3.577 g (58%). ^1H NMR ($CDCl_3$): 8.31 (d, 4H), 8.05 (d, 4H), 4.33 (t, 8H), 1.79 (m, 8H), 1.25-1.45 (m, 88H), 0.88 (t, 12H).

2.15. Thionation of 1,8-Naphthalic Anhydride

To confirm that phosphorus species observed in the XPS were a result of byproduct contamination, rather than chemical incorporation to the perylene, a control experiment of thionation of 1,8-naphthalic anhydride with P_4S_{10} was conducted using modifications of established procedures.[23-25] Anhydrides have not been thionated with P_4S_{10} in the literature; published syntheses are all conducted with LR. To confirm that P4S10 performs this transformation without forming phosphorus-carbon bonds to the thionated substrate, the thionation of 1,8-naphthalic anhydride was performed on a gram scale as described below.

1 g 1,8-naphthalic anhydride was dried in a flask on the Schlenk line, backfilled with Ar, and transferred to the flushbox. In the flushbox, 640 mg P_4S_{10} was added to the flask, along with a stir bar. The flask was fitted with a condenser, sealed with septa, and transferred back to the Schlenk line. After three pump-purge cycles with Ar to remove residual oxygen and water from the powders and interior atmosphere, 40 mL of chlorobenzene was added by syringe, and the flask was heated to reflux in an oil bath. The solution turned pale yellow as the naphthalic anhydride dissolved and steadily turned reddish-gold over the first few hours of reaction. After maintaining reflux conditions overnight, the solution was dark red, in good agreement with literature observations. The flask was cooled in an ice bath to precipitate product. The solid was then added to 40 mL ethanol, and the solution was boiled for one hour. After letting the ethanol evaporate overnight, the solid was dissolved in DCM and filtered through a plug of silica (1″ × 5″) to remove phosphorus oxides and phosphonates. The DCM was

evaporated to produce the product solid. ^{31}P NMR revealed no signal in ^{1}H coupled or ^{1}H decoupled spectra, while ^{1}H NMR revealed peaks indicative of thionated product as reported in the literature.

*2.16. Formation of Mercaptosilane Surfaces (**6**)*

To expand comparisons of organosulfur surfaces beyond thioanhydride and thioester surfaces, mercaptopropylsilane-functionalized surfaces were prepared by a literature procedure.[33] Briefly, 600 μL 3-mercaptopropyltrimethoxysilane was dissolved in 15.6 mL 2-propanol and 600 μL water to form a mercaptosilane solution. Oxidized silicon surfaces (**1**) were then subjected to three cycles of the following procedure:

1. Immersion in 1-2 mL of mercaptosilane solution in a 100 ˚C oil bath for 10 minutes,
2. Removal from solution and rinsing in 2-propanol,
3. Drying with an Ar stream, and
4. Annealing on a 100 ˚C hot plate for 8 minutes.

After three cycles, the substrates were again rinsed in 2-propanol, dried with an Ar stream, and stored until further use.

3. Results

3.1. Studies 1 and 2: Formation of Aminosilane Surfaces and Attachment of Perylene to Aminosilane Surfaces

PTCDA was attached through a reactive perylene intermediate to amine-functionalized substrates. The "activated" acid-ester perylene that forms from the DBU-catalyzed ring opening reaction is much more reactive to imide conversion at the surface amines, facilitating ring-closure and surface tethering of the perylene species.[20]

The infrared spectra in Fig. 7 and photoelectron spectra in Fig. 8 support the covalent attachment of perylene to the amine-functionalized surfaces. Perylene attachment was confirmed by presence of imide and phenyl features in the IR spectra (Figure 7) as well as presence of carbon, oxygen, and nitrogen in the XP spectra after heating to 200 °C in the UHV chamber of the XPS (5×10^{-9} torr) for an hour. Such conditions typically encourage desorption of almost all adventitious carbon and oxygen on substrates and result in a massively decreased carbon and oxygen signal. However, the heating study showed that carbon, oxygen, and nitrogen signals persist (Figure 8); we assign these signals to the perylene molecule in robust chemical attachment to the silanes on the surface through the formation of imide covalent bonds.

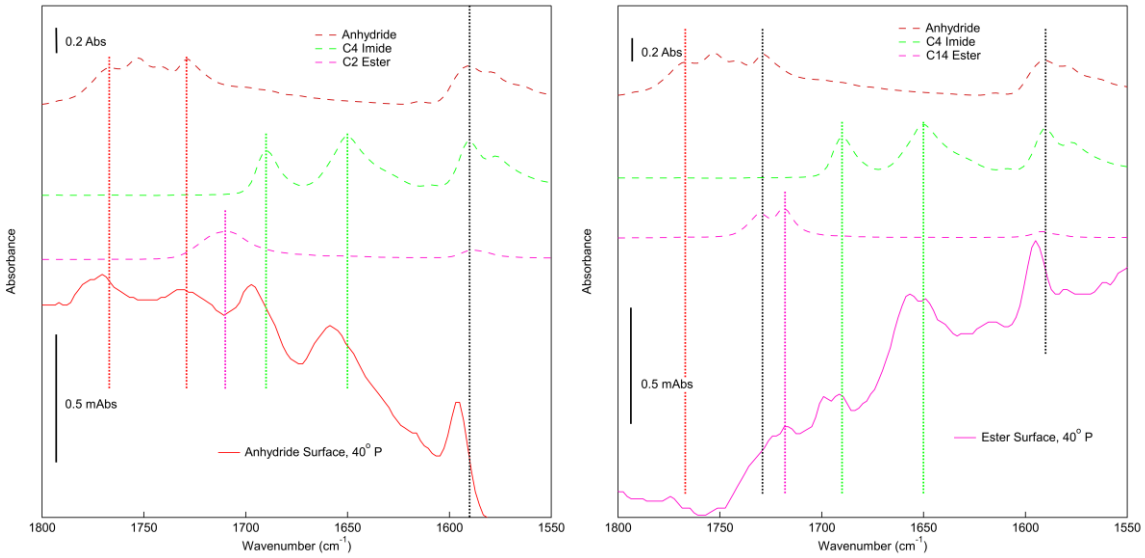

Figure 7: Carbonyl region of the IRRAS spectrum of surfaces **3a** (left) and **5a** (right) at 40° with respect to the surface normal in P polarization, with subtracted backgrounds of silane surface **2**. Powder IR scans of perylene reference molecules at the top of each spectrum guide peak assignments. Left: anhydride surface **3a**. Right: ester surface **5a**. Features at 1594 cm^{-1}, consistent across all reference molecules and surfaces, are assigned to phenyl C-C skeletal vibrations. Imide features at 1650 cm^{-1} and 1690 cm^{-1} indicate attachment of the perylene molecule to the surface amine. Symmetric and asymmetric anhydride C=O stretches are evident for surface **3a** at 1730 cm^{-1} and 1770 cm^{-1}. Ester C=O stretches are evident for surface **5a** at 1718 cm^{-1} and 1730 cm^{-1}. Though the peak at 1730 cm^{-1} in surface **4a** may indicate anhydride or ester C=O stretches, the presence of a peak at 1718 cm^{-1} and lack of a resolvable peak at 1770 cm^{-1} indicates ester character. Scale bars at left of figure show that surface IR features are on the order of ~0.5 milliabsorbance units, while features in references molecules are on the order of 0.2-0.4 absorbance units.

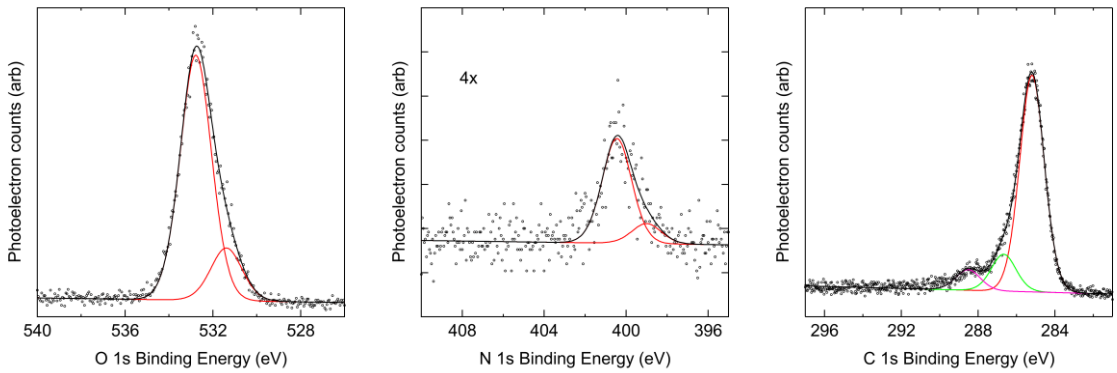

Figure 8: High-resolution XP spectra of the O 1s (left), N 1s (center), and C 1s (right) regions of surface **3a** following heating at 200 ˚C in the UHV chamber of the XPS for an hour. The *y*-axes are to scale between the C 1s and O 1s regions, and the N 1s region is respectively scaled 4×. The N 1s region reveals two features at 400.5 eV and 399.0 eV that we collectively assign to the imide and the aminopropyl silane. The C 1s region contains several organic carbon features in various oxidation states, at 285.2, 286.7, and 288.5 eV.

3.2. Study 3: Thionation of Surface Carbonyls

Once perylene was attached to substrates, thionation procedures could be optimized based only on the solubility and effectiveness of the thionating reagents at mild temperatures. The desired reaction conditions would involve relatively low temperatures to avoid damaging the electronic properties of single-crystalline substrates in future work.

For the conversion of surface **3a** to **3b**, surface thionation procedures initially utilized LR in refluxing chlorobenzene for 16 hours, following literature procedures for thionation of naphthalic anhydride in solution.[23-25] Instead of sulfide species corresponding to newly formed C=S bonds on the surfaces, XPS studies observed oxidized sulfur and phosphorus species. However, other publications on the use of LR mention its instability at temperatures above 110 ˚C, decomposing or polymerizing in solution;[26,34] therefore, we suspected that LR was decomposing over the prolonged reaction time in refluxing solution. Subsequent thionation procedures at 110 ˚C on surfaces using LR also yielded oxidized sulfur and phosphorus species in the XPS that were not removed by brief acid etches. Contamination of the chlorobenzene solution by dissolved water, which would have immediately reacted with LR, would likely have contributed only minimally to this decomposition as the chlorobenzene was purchased at an extra dry quality and stored under inert gas.

Based on the unsuitability of thionation via LR in refluxing chlorobenzene or toluene, the thionation procedure was changed to room-temperature flushbox conditions over a longer reaction time. Reaction conditions tested included:

1. P_4S_{10} in DCM at room temperature for 3 days
2. P_4S_{10} in toluene at room temperature for 3 days
3. LR in toluene at room temperature for 3 days
4. A P_4S_{10}-pyridine complex in pyridine at room temperature for 3 days

DCM and toluene were investigated as possible solvent choices for P_4S_{10} and compared to LR and a P_4S_{10}-pyridine complex, two alternative thionating reagents, in a parallel experiment at room temperature for 3 days in the flushbox, followed by extensive airfree rinsing and sonication to remove decomposition products from thionating reagents.

Figure 9 presents the S 2s and P 2p regions of a characteristic spectrum for surface **3b** after thionation procedures with various thionating reagents. We utilize the S 2s region rather than the more traditional S 2p region to minimize overlapping interference from silicon phonon-loss photoelectrons. The S 2s spectrum demonstrates features at ~228 and ~229 eV that we ascribe to covalent organic sulfur species with no detectable contribution of oxidized sulfur species that we would expect at 232-235 eV.[32] In contrast to the sulfur spectrum, the P 2p region demonstrates features ascribed to highly oxidized phosphorus species. Importantly, the integrated areas of the S 2s to P 2p regions (termed the S:P ratio) show significant improvement over previous thionation attempts, with a sulfur signal far above the noise (Figure 9). The corrected S:P ratio, after adjusting for instrument-specific sensitivity factors,[32] was 5.5 ± 1.0 for the best-performing thionation scheme – P_4S_{10} in toluene (Table 1). The integrated areas of the S 2s to N 1s regions (termed the S:N ratio) show improved coverage of sulfur on the surface to a S:N ratio of 2.3 ± 0.3 when using P_4S_{10} in toluene as well.

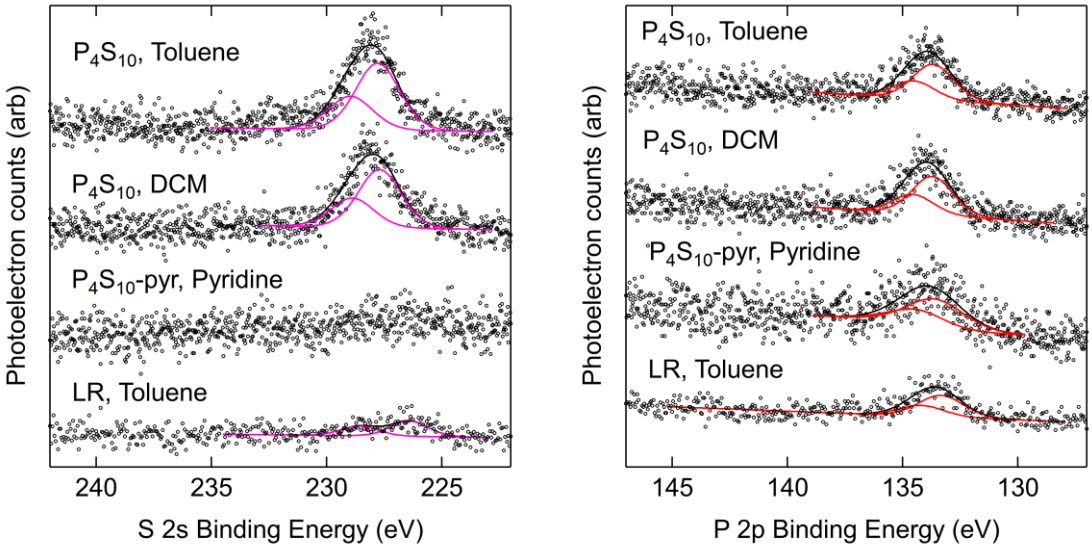

Figure 9: High-resolution XP spectra of the S 2s (left) and P 2p (right) regions for the four thionation procedures studied. Surface sulfur species were maximized for reaction procedures with P_4S_{10}, with only trace features present for reactions with LR or a pyridine-P_4S_{10} complex. The position of the sulfur features (228 eV, magenta) corresponds to sulfide species, rather than oxidized sulfur species that would appear between 232-235 eV. Oxidized phosphorus features (red) are present at ~134 eV for all reaction conditions due to unwanted decomposition byproducts from the thionation reaction. These byproducts were minimized using an extensive airfree sonication procedure (see *2.12*) in aromatic solvents.

Thionation Scheme	S:P Ratio	S:N Ratio	Number of Substrates
P_4S_{10}, toluene	5.5 ± 1.0	2.3 ± 0.3	3
P_4S_{10}, DCM	4.1	1.6	1
P_4S_{10}–pyridine complex, pyridine	1.0	0.49	1
LR / toluene	1.5 ± 1.2	0.23 ± 0.07	3

Table 1. Sensitivity-adjusted XPS integrated area ratios of sulfur to phosphorus and sulfur to nitrogen for each thionation reaction scheme studied. P_4S_{10} in toluene and dichloromethane performed the best of the three thionation reagents studied, as defined by a high ratio of organosulfur to oxidized phosphorus and high ratio of organosulfur to aminosilane nitrogen. The addition of the perylene molecules on top of the aminosilane attenuates the nitrogen signal, as the photoelectrons from the nitrogen atoms must pass through the organic layer to be detected; this effect is not accommodated for in the calculation of the S:N area ratio. Instrument-specific element sensitivity factors were applied to compare the relative atomic ratios of S:P and S:N.

3.3. Study 4: Deposition of Metal Sulfides

Antimony sulfide (Sb_2S_3) was deposited onto various surfaces by a literature procedure by Savadogo & Mandal,[11] using antimony potassium tartrate as the antimony source and thioacetamide as the sulfur source. The films were characterized by XPS (Figure 10) immediately following a 10-second etch in 10% aqueous HCl. The films consist mainly of Sb_2S_3 based on the positions of the antimony and sulfur peaks in the XPS. The peaks at 532.0 eV and 533.0 eV (orange) are assigned to oxygen species from the overlapping O 1s region, while the rest of the peaks in the Sb 3d spectrum are assigned to antimony. The three peaks for antimony correspond to trace partial oxide or sesquioxide at 531.0 eV (green), sulfide at 529.9 eV (magenta), and antimony metal at 528.2 eV (red). The metallic Sb^0 feature is due to X-ray damage from the instrument. The doublet in the sulfur spectrum at 161.8 eV (magenta) matches well with literature values for metal sulfides. The small doublet in the sulfur spectrum at 163.0 eV (green) is assigned to slightly oxidized sulfur species, possibly due to some interfacial sulfur atoms reacting with ambient oxygen or water to form S=O or S–OH surface species. The absence of observable higher binding energy features indicates at most minimal formation of highly oxidized interfacial sulfur species.

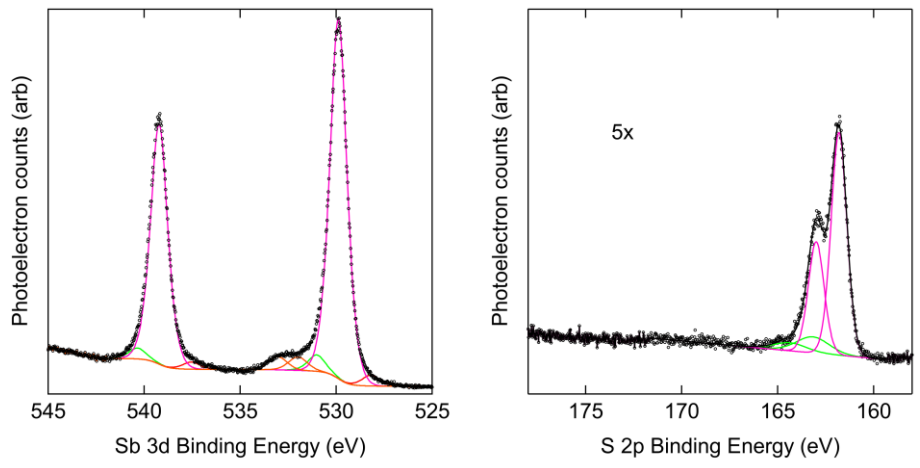

Figure 10: High-resolution XP spectra of the Sb 3d region (left) and S 2p region (right) when scanning deposited Sb_2S_3 thin films, with the S 2p region scaled 5x vertically. The O 1s and Sb 3d regions overlap, so two O 1s features are visible at 532.0 eV and 533.0 eV (orange). Sulfide (529.9 eV and 539.2 eV, magenta) and sesquisulfide (531.0 eV and 540.4 eV, green) indicate high purity material. Some metallic Sb (528.2 eV and 537.5 eV, red) is present due to X-ray beam damage, occasionally observed when examining sulfides. The S 2p region indicates high purity material through a large sulfide doublet at 161.8 eV and 163.0 eV (magenta), with a small partially oxidized sulfur at 163.2 eV and 164.4 eV (green).

3.4. Photoelectrochemistry of Antimony Sulfide

The performance of the thionated perylenes as electron transport layers for the Si - Sb_2S_3 system was tested with photoelectrochemistry using the thianthrene$^{+/0}$ redox couple in acetonitrile. The stability of the redox couple was tested beforehand using a silver wire electrode in $AgNO_3$ solution, also in acetonitrile. Ferrocene$^{+/0}$ and acetylferrocene$^{+/0}$ redox couples were added to the solution to further calibrate the position of the thianthrene$^{+/0}$ redox couple with reference to ferrocene$^{+/0}$. Figure 11 presents the cyclic voltammogram with potential calibrated vs that of ferrocene$^{+/0}$, in which thianthrene$^{+/0}$ was measured as 820 mV more oxidizing than ferrocene $^{+/0}$. This value compares favorably with the literature value of 860 mV,[35] as differences in supporting electrolyte can cause slight shifts in potential.

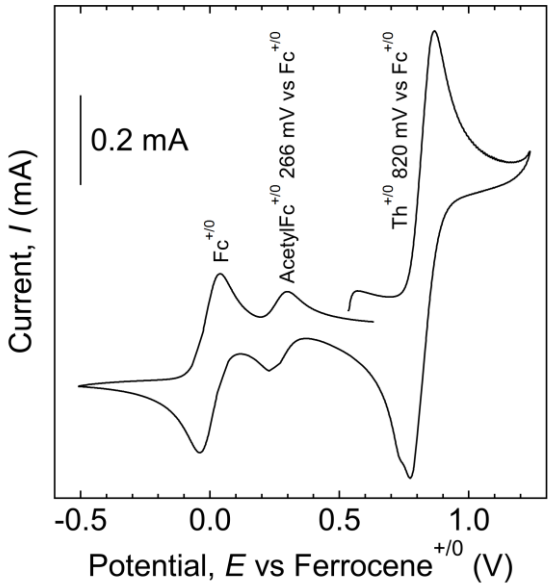

Figure 11: Cyclic voltammogram of 119 mg thianthrene / ~4 mg thianthrene tetrafluoroborate ($Th^{+/0}$), in acetonitrile, with reference features for ferrocene ($Fc^{+/0}$) and acetylferrocene ($AcetylFc^{+/0}$) redox couples with identical counterions. $LiClO_4$ (1M) was used as electrolyte. Potentials were measured in reference to the $Ag^{+/0}$ and transformed to depict potential vs ($Fc^{+/0}$). The strongly oxidizing potential of $Th^{+/0}$ is measured at 820 mV vs $Fc^{+/0}$.

Following calibration, the thianthrene$^{+/0}$ redox couple was used to measure open-circuit voltages from Sb_2S_3 films deposited on surfaces **1**, **2**, **3a**, **3b**, **4a**, **4b**, and **6**. Figure 12 and Table 2 present the results of open-circuit voltage (V_{oc}) experiments, in which the substrate was illuminated beginning approximately five seconds into the scan. Notably, Sb_2S_3 absorbers on thioanhydride surfaces (**3b**) exhibit increased V_{oc} compared to their

sulfur-free counterpart **3a**, yet thioester **4b** failed to outperform ester surfaces **4a**. Sb_2S_3 absorbers on aminosilane (**2**) and mercaptosilane control surfaces (**6**) exhibit poor V_{oc}. Sb_2S_3 absorbers on thioanhydride surfaces (**3b)** exhibit excellent open-circuit voltages of ~–900 mV for the best-performing electrodes.

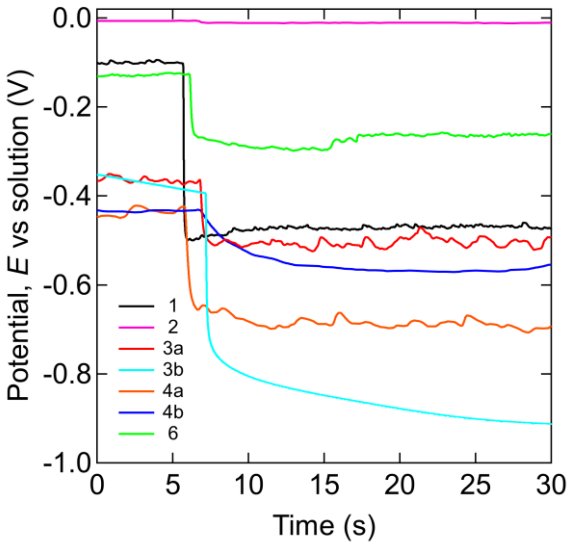

Figure 12: V_{oc} scans of Sb_2S_3-deposited surfaces **1**, **2**, **3a**, **3b**, **4a**, **4b**, and **6** with illumination beginning at time = ~5 seconds. These scans represent the highest V_{oc} collected for each surface category. All surfaces displayed exhibit light/dark response. Sb_2S_3 on thioanhydride surface **3b** (teal) shows improved voltage over Sb_2S_3 on anhydride surface **3a** (red), yet thioester surface **4b** (blue) does not provide improved voltage over ester surface **4a** (orange) for Sb_2S_3. Sb_2S_3 performs comparably on plain oxidized surfaces **1** (black) and anhydride **3a**, while aminosilane **2** (magenta) and mercaptosilane **6** (green) surfaces exhibit poor voltages.

Electrode Setup	$\lvert V_{oc} \rvert$ (mV)	Number of Electrodes
Sb_2S_3 / **1** / n^+-Si	380 ± 160	5
Sb_2S_3 / **2** / n^+-Si	8 ± 6	2
Sb_2S_3 / **3a** / n^+-Si	380 ± 140	5
Sb_2S_3 / **3b** / n^+-Si	650 ± 190	7
Sb_2S_3 / **4a** / n^+-Si	500 ± 200	5
Sb_2S_3 / **4b** / n^+-Si	300 ± 200	5
Sb_2S_3 / **6** / n^+-Si	220 ± 110	4

Table 2. Performance of Sb_2S_3 deposited on surfaces **1**, **2**, **3a**, **3b**, **4a**, **4b**, and **6** by open-circuit voltage (V_{oc}), measured with the thianthrene$^{+/0}$ redox couple. The V_{oc} values were highest for thioanhydride surfaces **3b**. Current densities are not reported due to poor solubility of the thianthrene charge carrier species in acetonitrile.

4. Discussion

4.1. Studies 1 and 2: Formation of Aminosilane Surfaces and Attachment of Perylene to Aminosilane Surfaces

The formation of the aminosilane monolayer is already a well-established field of study in the literature.[22,36] The attachment of perylene through the soluble di-acid di-ester proceeded to high enough coverages for observation in the carbonyl region of the IR (Figure 7) including separate peaks for imide and anhydride moieties.

Further modification of **3a** to **4a** was possible from mild reaction conditions overnight, as evident from peak shifts in the carbonyl region from anhydride to ester positions, while maintaining imide features (Figure 7). Extending the ester alkyl group from ethyl to tetradecyl by formation of **5a** was expected to result in more prevalent C-H stretches in the aliphatic region of the IR to confirm conversion to ester groups beyond carbonyl stretches; however, scans of the C-H region were inconclusive. In any case, longer alkyl chains are unlikely to prove relevant to tandem solar cell development, as more hydrophobic surfaces would likely hinder aqueous metal sulfide depositions by affecting adhesion of the films. Ethyl alkyl groups allow room-temperature formation of the esters by use of bromoethane; proceeding to a methyl alkyl group would require either lower temperatures to accommodate the lower boiling point of methyl bromide or use of the higher-boiling methyl iodide. The methyl alkyl group would offer the least steric hindrance and least hydrophobic character to sulfur-functionalized ester surfaces; these properties may advantageously affect the performance of metal sulfides deposited on ester surfaces.

4.2. Study 3: Thionation of Surface Carbonyls

The position of the peaks in the S 2s XP spectra (Figure 8) corresponds to covalent organosulfur species.[32] We assign these features to C=S conversion by the thionating reagent. The phosphorus signal from deposited decomposition products of the thionating

reagents was comparable in integrated XPS area across multiple thionation reaction conditions, but in our hands the S:P ratio was maximized when using P_4S_{10} in toluene. The consistent phosphorus signal is indicative of persistent contamination by reactant byproducts.

There are four oxygens on the attached perylene species reactive toward thionating reagents: two anhydride carbonyl oxygens at the top and two imide carbonyl oxygens at the bottom. For high perylene coverages, to the extent that C=O stretches and C-C ring modes are visible in the IR (Figure 7), the presence of nearby perylene molecules likely sterically hinders the ability of thionating reagents to react with the imide oxygens. The presence of additional unreacted silanes likely also contributes to steric hindrance, as well as the proximity of the imide oxygens to the silicon surface. Steric hindrances were observed in the thionation reaction of N-alkyl imides in the literature, where tert-butyl, phenyl, and adamantyl groups drastically decreased thionation yields.[37] The proximity of the silicon surface only compounds the expected sterics. Therefore, we assign the organosulfur signal to thionated anhydride carbonyls.

Despite observable sulfur signal in the XPS, we were unable to identify C=S modes in surface IR scans (1250–1050 cm^{-1}) that would indicate thiocarbonyl conversion. We attribute the lack of visible peaks in those regions to the weaker oscillation of C=S vs C=O; as is, C=O modes were on the order of 0.5 milliabsorbance units in the surface IR. Similar absorbance magnitudes have been reported for carbonyl stretches by our group.[38] Additionally, transverse-optical (TO) and longitudinal-optical (LO) modes corresponding to silicon-oxygen bonds complicate the 1200–1000 cm^{-1} region of the spectrum, as slow formation of oxide in the silicon substrate likely results in peaks even after background subtraction.

This study chose to optimize thionation procedures for room temperature conditions. In preliminary thionation procedures, the solubility of thionating reagents such as LR and P_4S_{10} was observed to change drastically with temperature for aromatic

solvents such as toluene and chlorobenzene. Further studies may investigate increasing temperatures to increase the solubility of the thionating reagents, while avoiding conditions harmful to silicon substrates. Other solvents that have been used for thionation procedures in the literature, such as chlorobenzene, diglyme, acetonitrile, or tetrahydrofuran, could also be investigated.

4.3. Study 4: Deposition of Metal Sulfides

Two Sb_2S_3 depositions, with Ar annealing after each deposition, resulted in high purity films as observed in the XPS (Figure 11) and high V_{oc} from films deposited on thioanhydride surfaces **3b** (Figure 12). To our knowledge, the highest V_{oc} measured, approximately –900 mV, is the highest V_{oc} reported for Sb_2S_3 films. The large V_{oc} is attributed partly due to the extremely oxidizing potential of the thianthrene$^{+/0}$ redox couple, partly due to the electronic properties of perylene molecules on the surfaces, and partly due to the thionation procedures studied in this work.

The thianthrene$^{+/0}$ redox couple was measured at a potential 820 mV more oxidizing than the conventional ferrocene$^{+/0}$ redox couple. This position allows carrier separation upon generation of photo-excited states, as electron holes are removed by the thianthrene$^{+/0}$ redox couple while electrons flow through the perylene layer to be collected at the silicon / GaIn back. The carrier separation improves open-circuit voltages.

To determine the contributing factors behind the success of the thioanhydride, the results were compared to mercaptosilane (**6**) and anhydride (**3a**) control surfaces. The presence of sulfur at the surface to interact favorably with Sb_2S_3 forming during the deposition procedure is not the sole factor behind the high performance, as mercaptosilane surfaces performed poorly in V_{oc} experiments. The number of sulfur atoms at the surface is not a likely cause; the mercaptosilane reaction likely proceeds to higher coverages than perylene coverages, which suffer from steric constraints from the size of the perylene molecule once some perylenes have attached to the surface. Sulfide

(S^{2-}) character presented by the thioanhydride, rather than thiol (SH) character from the mercaptosilane, may contribute to better photovoltaic performance. This result merits additional future studies.

The hole-blocking properties of the surface perylenes may contribute to the success of the thioanhydride surfaces. Thionation of the anhydride carbonyls will likely shift the valence and/or conduction band positions of the perylene anhydride, similar to observations in UV-Vis spectra of thionated perylene diimides in prior literature.[18,19] As-is, anhydride surfaces (**3a)** performed comparably to oxidized surfaces (**1**) in V_{oc} measurements. Exposed carbonyl oxygens, rather than thiocarbonyl sulfurs, may hinder sulfide deposition procedures or deposited sulfide performance. Alternatively, the valence and/or conduction bands of the perylene on the surface may not be optimally positioned to improve photovoltaic properties of the silicon – Sb_2S_3 system.

Ester surfaces (**4a**) produced acceptable V_{oc} values for deposited Sb_2S_3, while thioester surfaces (**4b**) produced noticeably lower voltages. The low voltages may be due to poor adherence, as ester groups present a more hydrophobic surface in the chemical bath solution due to carbon chains. The ethyl alkyl group on the esters may be shortened to methyl alkyl groups in future work to mitigate the nonpolar CH presence on surfaces. Another possibility is that the esterification procedure shifts the perylene conduction and/or valence bands to positions that aid carrier separation, while thionation of the esters upsets the band positions from this state.

5. Conclusions and Future Work

A variety of surface perylene species were prepared on oxidized silicon surfaces through aminosilane attachment and further modification by organic reactions. These surfaces were deposited with antimony sulfide (Sb_2S_3) by chemical bath deposition procedures and studied by photoelectrochemistry to determine pathways to improved solar absorber performance. Thionated perylene surfaces were prepared and investigated in an effort to provide sulfur-containing surfaces that may provide favorable surfaces for deposition of metal sulfides. Thioanhydride perylene derivatives exhibited improved photovoltaic performance over anhydride derivatives, while thioester derivatives failed to outperform sulfur-free ester surfaces. Sb_2S_3 deposited on mercaptosilane control surfaces performed worse than unmodified oxidized silicon surfaces, indicating that presence of sulfur is not sufficient to improve deposition. Thioanhydride surfaces performed the best of all surfaces studied, generating a world record –900 mV open-circuit voltage for Sb_2S_3 thin films.

While this work has produced promising results that contribute to antimony sulfide's future as a solar absorber candidate, several properties of the attached perylene species are still unknown. The band positions of the perylene molecule attached to the surface, as well as the shifts in band positions that occur upon thionation or esterification, were not determined in these studies. Future studies using ultraviolet photoelectron spectroscopy and UV-Vis surface spectroscopy could measure these optical properties. Addition of substituents to the "bay" positions of the perylene core will also shift bands, so future work could determine optimal R– groups by synthesizing and attaching various derivatives of PTCDA and testing their optical and carrier transport properties.

Future experiments may vary perylene ester alkyl chain length to assess the effect of surface polarity on deposited Sb_2S_3 thin films. Further modification of the thioanhydride surfaces to trithioanhydride surfaces is possible and may be investigated as a method of increasing sulfur coverage.

6. References

1. Retrieved from https://www.nrel.gov/pv/cell-efficiency.html. This plot is courtesy of the National Renewable Energy Laboratory, Golden, CO.
2. Shockley, W.; Queisser, H.J. Detailed balance limit of efficiency of p-n junction solar cells. *J. Appl. Phys.* **1961,** *32,* 510-519.
3. Grimm, R.L. Department of Chemistry and Biochemistry, Worcester Polytechnic Institute, Worcester, MA. Personal communication, July 2018.
4. Kondrotas, R.; Chen, C.; Tang, J. Sb_2S_3 solar cells. *Joule* **2018,** *2,* 857-878.
5. Lewis, D.J.; Kevin, P.; Bakr, O.; Muryn, C.A.; Malik, M.A.; O'Brien, P. Routes to tin chalcogenide materials as thin films or nanoparticles: a potentially important class of semiconductor for sustainable solar energy conversion. *Inorg. Chem. Front.* **2014,** *1,* 577.
6. Zhou, X.; Zhang, Q.; Gan, L.; Li, H.; Xiong, J.; Zhai, T. Booming development of group IV-VI semiconductors: fresh blood of 2D family. *Adv. Sci.* **2016,** 1600177.
7. Chaki, S.H.; Chaudhary, M.D.; Deshpande, M.P. SnS thin films deposited by chemical bath deposition, dip coating and SILAR techniques. *J. Semicond.* **2016,** *37*(5), 053001.
8. Messina, S.; Nair, M.T.S.; Nair, P.K. Antimony sulphide thin film as an absorber in chemically deposited solar cells. *J. Phys. D: Appl. Phys.* **2008,** *41,* 095112.
9. Sreedevi, G.; Reddy, K.T.R. Properties of tin monosulphide films grown by chemical bath deposition. *Conference Papers in Energy* **2013**, 528724.
10. Lokhande, C.D. A chemical method for tin disulphide thin film deposition. *J. Phys. D: Appl. Phys.* **1990,** *23,* 1703-1705.
11. Savadogo, O.; Mandal, K.C. Characterizations of antimony tri-sulfide chemically deposited with silicotungstic acid. *J. Electrochem. Soc.* **1992,** *139*(1), L16-L18.
12. Fujisawa, J.-I.; Eda, T.; Hanaya, M. Comparative study of conduction-band and valence-band edges of TiO_2, $SrTiO_3$, and $BaTiO_3$ by ionization potential measurements. *Chem. Phys. Lett.* **2017,** *685,* 23-26.
13. Huang, C.; Barlow, S.; Marder, S.R. Perylene 3,4,9,10-tetracarboxylic acid diimides: synthesis, properties, and use in organic electronics. *J. Org. Chem.* **2011,** *76,* 2386-2407.
14. Nagao, Y. Synthesis and properties of perylene pigments. *Prog in Org. Coatings* **1997,** *31,* 43-49.
15. Dubey, R.K.; Westerveld, N.; Eustace, S.J.; Sudholter, E.J.R.; Grozema, F.C.; Jager, W.F. Synthesis of Perylene-3,4,9,10-tetracarboxylic Acid Derivatives Bearing Four Different Substituents at the Perylene Core. *Org. Lett.* **2016,** *18*(21), 5648-5651.
16. Vajiravelu, S.; Ramunas, L.; Vidas, G.J.; Valentas, G.; Vygintas, J.; Valiyaveettil, S. Effect of substituents on the electron transport properties of bay substituted perylene diimide derivatives. *J. Mat. Chem.* **2009,** *24,* 4268-4275.
17. Sengupta, S.; Dubey, R.K.; Hoek, R.W.M.; van Eeden, S.P.P.; Gunbas, D.D.; Grozema, F.C.; Sudholter, E.J.R.; Jager, W.F. Synthesis of regioisomerically pure 1,7-Dibromoperylene-3,4,9,10-tetracarboxylic acid derivatives. *J. Org. Chem.* **2014,** *79,* 6655-6662.
18. Tilley, A.J.; Pensack, R.D.; Lee, T.S.; Djukic, B.; Scholes, G.D.; Seferos, D.S. Ultrafast triplet formation in thionated perylene diimides. *J. Phys. Chem. C* **2014,** *118,* 9996-10004.
19. Llewellyn, B.A.; Davies, E.S.; Pfeiffer, C.R.; Cooper, M.; Lewis, W.; Champness, N.R. Thionated perylene diimides with intense absorbance in the near-IR. *Chem. Commun.* **2016,** *52,* 2099-2102.

20. Kelber, J.; Bock, H.; Thiebaut, O.; Grelet, E.; Langhals, H. Room-temperature columnar liquid-crystalline perylene imido-diesters by a homogenous one-pot imidification-esterification of perylene-3,4,9,10-tetracarboxylic dianhydride. *Eur. J. Org. Chem* **2011,** *4*, 707-712.
21. Carl, A.D.; Kalan, R.E.; Obayemi, J.D. Zebazi, M.G.; Soboyejo, W.O.; Grimm, R.L. Synthesis and characterization of alkylamine-functionalized Si(111) for perovskite adhesion with minimal interfactial oxidation or electronic defects. *ACS Appl. Mater. Interfaces* **2017,** *9,* 34377-34388.
22. Zhu, M.; Lerum, M.Z.; Chen, W. How to prepare reproducible, homogeneous, and hydrolytically stable aminosilane-derived layers on silica. *Langmuir* **2012,** *28,* 416-423.
23. Lakshmikantham, M.V.; Chen, W.; Cava, M.P. Thionahydrides. 3. Synthesis, properties, and Diels-Alder reactions of sulfur analogues of 1,8-naphthalic anhydride. *J. Org. Chem.* **1989,** *54,* 4746-4750.
24. Huang, T.; Qian, X.; Tao, Z.; Wang, K.; Song, G.; Liu, L. The improved synthesis, Diels-Alder reactions, and desulfuration of trithio-1,8-naphthalic anhydride. *Heteroatom Chem.* **1999,** *10,* 141-146.
25. Huang, T.; Zhang, J.; Zhu, D.; Yao, W.; Qian, X. General synthesis of thioxo-1,8-naphthalimdes via thioxo-1,8-naphthalic anhydrides. *Synthesis* **1999,** *7,* 1109-1111.
26. Ozturk, T.; Ertas, E.; Mert, O. Use of Lawesson's reagent in organic syntheses. *Chem. Rev.* **2007,** *107,* 5210-5278.
27. Ozturk, T.; Ertas, E.; Mert, O. A Berzelius reagent, phosphorus decasulfide (P_4S_{10}) in organic syntheses. *Chem. Rev.* **2010,** *110,* 3419-3478.
28. Bergman, J.; Pettersson, B.; Hasimbegovic, V. Svensson, P.H. Thionations using a P_4S_{10}-pyridine complex in solvents such as acetonitrile and dimethyl sulfone. *J. Org. Chem.* **2011,** *76,* 1546-1553.
29. Kingi, N.; Bergman, J. Thionation of tryptanthrin, rutaecarpine, and related molecules with a reagent prepared from P_4S_{10} and pyridine. *J. Org. Chem.* **2016,** *81,* 7711-7716.
30. Masucci, C. P. (2018). *Photoelectrochemistry of n-Silicon and Bismuth(III) Iodide*. Retrieved from https://digitalcommons.wpi.edu/mqp-all/4098.
31. Boduszek, B.; Shine, H.J. Preparation of solid thianthrene cation radical tetrafluoroborate. *J. Org. Chem.* **1988,** *53,* 5142-5143.
32. Moulder, J.F.; Stickle, W.F.; Sobol, P.E. Bomden, K.D. *Handbook of X-ray photoelectron spectroscopy: A reference book of standard spectra for identification and interpretation of XPS data;* Chastain, J., Ed.; Perkin-Elmer Co: Eden Prairie, MN, 1992.
33. Matisons, J.G. *Silanes and siloxanes as coupling agents to glass: a perspective.* In: Owen M., Dvornic P. (eds) Silicone Surface Science. Advances in Silicon Science, vol 4. Springer, Dordrecht, **2012.**
34. Voss, J. 2,4-bis(4-methoxyphenyl)-1,3,2,4-dithiadiphosphetane 2,4-disulfide. *Encyclopedia of Reagents for Organic Synthesis,* 2006.
35. Connelly, N.G.; Geiger, W.E. Chemical redox agents for organometallic chemistry. *Chem. Rev.* **1996,** *96*(2), 877-910.
36. Ulman, A. Formation and structure of self-assembled monolayers. *Chem. Rev.* **1996,** *96,* 1533-1554.
37. Orzeszko, A.; Maurin, J.K.; Melon-Ksyta, D. Investigation of the thionation reaction of cyclic imdes. *Z. Naturforsch* **2001,** *56b,* 1035-1040.
38. Carl, A.D.; Grimm, R.L. Covalent attachment and characterization of perylene monolayers on Si(111) and TiO_2 for electron-selective carrier transport. In preparation.

7. Appendix

7.1. NMR of Synthesized Perylene Derivatives

^{1}H NMR spectra are reported for perylene-3,4,9,10-tetracarboxylic tetraethyl ester (Figure A1) as well as perylene-3,4,9,10-tetracarboxylic tetratetradecyl ester in comparison to its tetradecyl reactants (Figure A2) below.

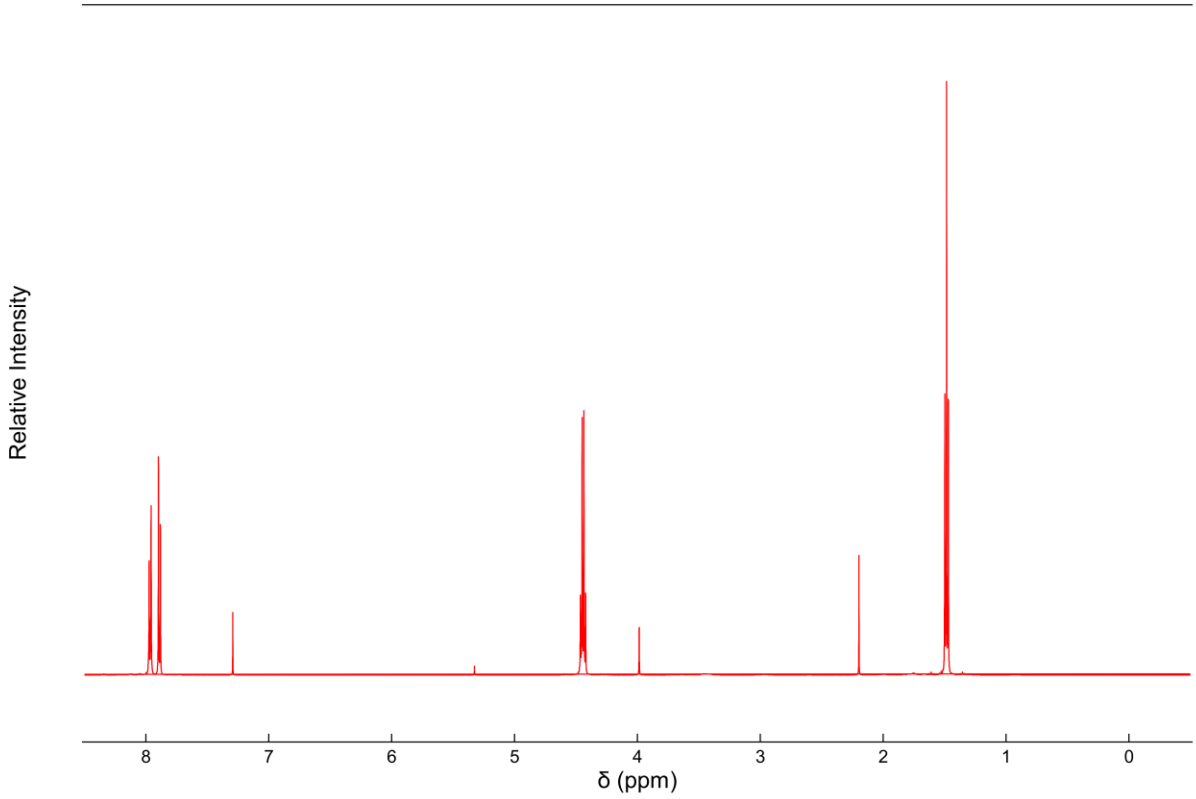

Figure A1: ^{1}H NMR spectra of perylene-3,4,9,10-tetracarboxylic tetraethyl ester. Aryl protons are evident at 7.8-8.0 ppm and the ethyl groups provide CH_2 protons at 4.4 ppm and CH_3 protons at 1.5 ppm. Various solvent impurities ($CHCl_3$, DCM, EtOH) are minimal.

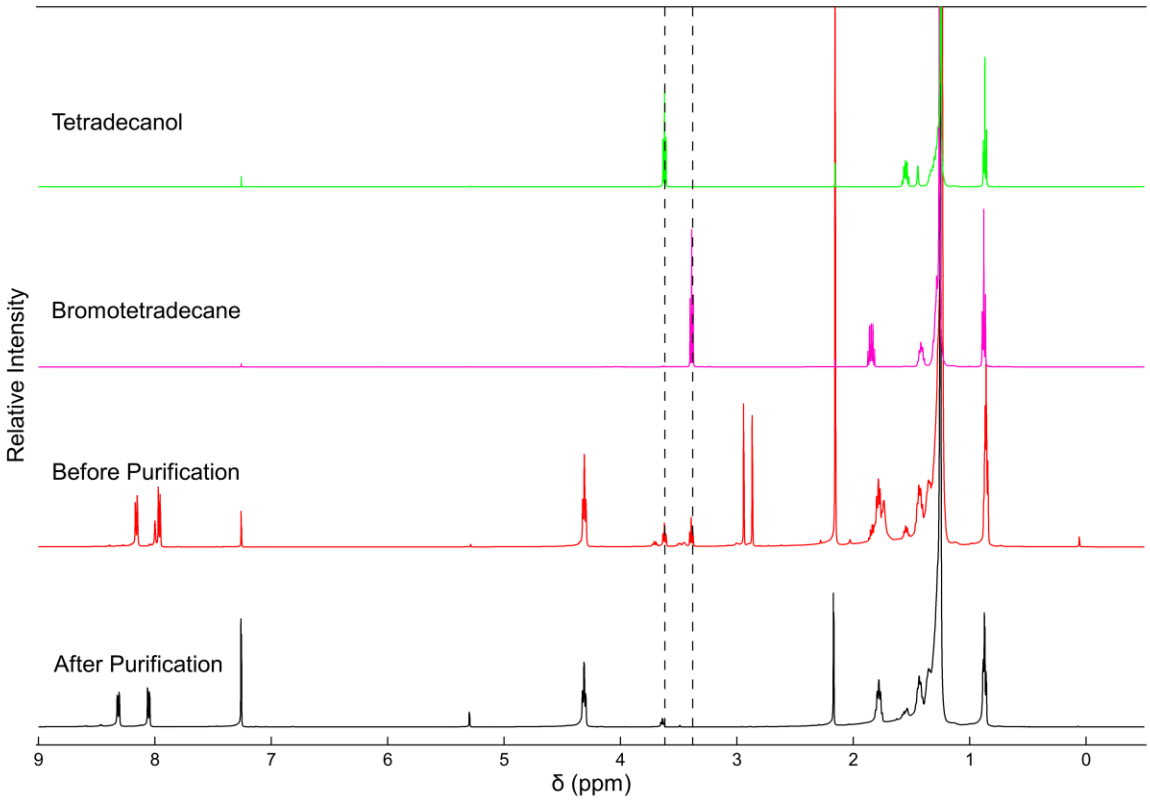

Figure A2: Stacked ^{1}H NMR spectra of crude (red) and purified (black) perylene-3,4,9,10-tetracarboxylic tetratetradecyl ester, with reference spectra of 1-tetradecanol (green) and 1-bromotetradecane (magenta) starting material, all collected on the same instrument. Impurities of the starting material, indicated by matching ppm shifts of alcohol and halogen protons at guideline positions, were present in the crude product but minimized after column chromatography.

7.2. Surface IR Spectra

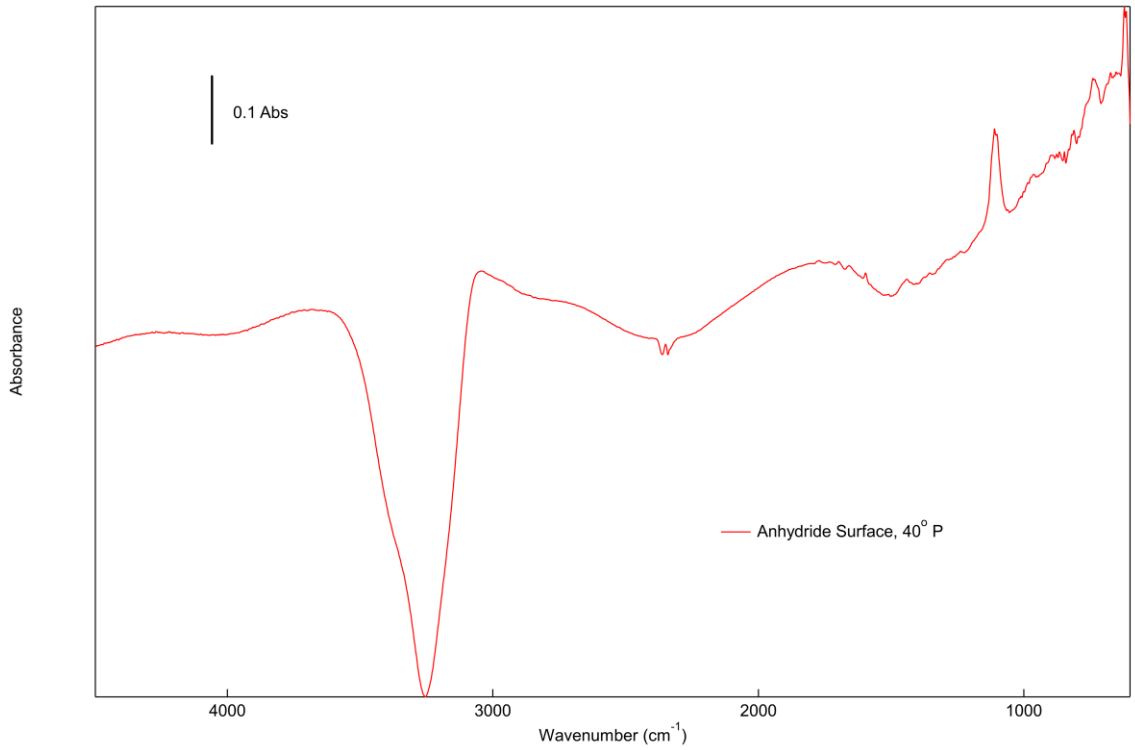

Figure A3: Complete surface IR spectrum of **3a**.

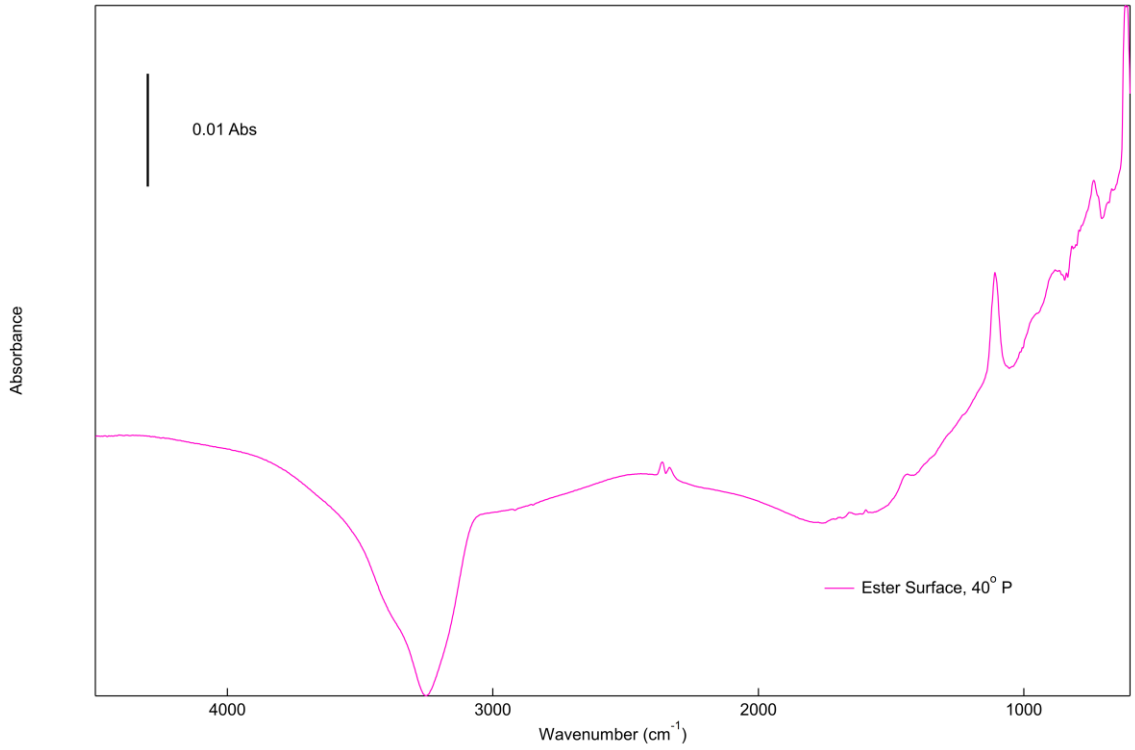

Figure A4: Complete surface IR spectrum of **4a**.